2018-01-01

Evaluation of Brackish Water Desalination by Membrane Capacitive Deionization Systems: Performance Tradeoffs in Salt Removal, Hydraulic Recovery, Charge Efficiency, and Specific Energy Consumption

Oluwaseye Michael Owoseni
University of Texas at El Paso, oaowoseni@gmail.com

EVALUATION OF BRACKISH WATER DESALINATION BY MEMBRANE CAPACITIVE DEIONIZATION SYSTEMS: PERFORMANCE TRADEOFFS IN SALT REMOVAL, HYDRAULIC RECOVERY, CHARGE EFFICIENCY, AND SPECIFIC ENERGY CONSUMPTION

OLUWASEYE MICHAEL OWOSENI

Doctoral Program in Civil Engineering

APPROVED:

W. Shane Walker, Ph.D., Chair

Anthony J. Tarquin, Ph.D.

Ivonne Santiago, Ph.D.

Rafael Verduzco, Ph.D.

Charles Ambler, Ph.D.
Dean of the Graduate School

Dedication

I dedicate this work to the Lord Almighty, for always being there for me even in my low estates.
To God be the Glory!

EVALUATION OF BRACKISH WATER DESALINATION BY MEMBRANE CAPACITIVE DEIONIZATION SYSTEMS: PERFORMANCE TRADEOFFS IN SALT REMOVAL, HYDRAULICRECOVERY, CHARGE EFFICIENCY, AND SPECIFIC ENERGY CONSUMPTION

by

OLUWASEYE MICHAEL OWOSENI, MSc

DISSERTATION

Presented to the Faculty of the Graduate School of

The University of Texas at El Paso

in Partial Fulfillment

of the Requirements

for the Degree of

DOCTOR OF PHILOSOPHY

Civil Engineering Department

THE UNIVERSITY OF TEXAS AT EL PASO

December 2018

Acknowledgements

Considering the opportunity given me to work on research that contributes to the alleviation of the impending water crisis around the globe, I cannot but express my appreciation. My sincere appreciation goes to my advisor, Dr. Shane Walker, for being of great support to me during this PhD journey, investing a tremendous amount of time and effort. I believe strongly that the Lord placed you on my path to be a mentor, a brother, a friend, and an inspiration. I also appreciate my Dissertation Committee; Dr. Anthony Tarquin, Dr. Ivonne Santiago, and Dr. Rafael Verduzco for their support through the completion of this dissertation.

I am grateful to the members of staff of the Center for Inland Desalination Systems (CIDS), most especially Dr. Malynda Cappelle for her support and prompt advice when needed. My sincere gratitude also goes to my mentors, friends, and colleagues in the water quality laboratory who helped me with running experiments, preparing materials and created hilarious moments that kept the mind sane throughout my graduate program. Thank you to Andres Sanchez, Avianna Gallegos, Cesar Alvarez, Clara Borrego, Daniela Hernandez, Denise Garcia, Francisco Solis, Frida Murga, Gabriela Porras, Isaac Campos, Juan Canales, Julio Gallegos, Katie Lee, Mackayla Thyfault, Martha Gonzalez, Miguel Fraga, Tallen Capt, and Troy Svede for making the water quality laboratory a family unit and a place to learn and gain knowledge on diverse matters.

I appreciate the contributions from Amit Jain from Rice University who collaborated on aqueous processed electrodes manufacturing; thank you for sharing your knowledge. My appreciation also goes to Andrew Barnett and Sophia Grossweiler for their input in developing the supervisory control and data acquisition system in LabVIEW. I appreciate Yair Morales who helped with introduction to Visual Basic for Application (VBA) coding in Microsoft Excel. Thank you to Uriel Lopez for his help in designing and fabricating the MCDI stack used in this research.

To my friend and brother, Shahrouz Jafarzade Ghadimi, having you by my side through this journey has been truly a blessing. Thank you for all the nights of endless brainstorming, thank you for your contributions to the model development, that truly came in handy. I am honored to have shared my time in the laboratory and outside the laboratory with you.

To my parents, Olugbenga and Mercy Owoseni, your relentless zeal, physical support, spiritual backing and countless sacrifices to ensure I and my other siblings reach our goals has been and continues to be a great pillar of support for us. Thank you, Dad, for pushing me to reach for higher grounds, though painful at times, it sure pays off in the end. Mom, you are indeed a rare jewel, my heart is overwhelmed with gratitude for your love and care. I appreciate the encouraging words and motivation of my siblings (Ibiwumi, Olasehinde, and Oluwanifemi), I am truly blessed to have you all. I cannot but appreciate my fiancée, Sidouane Patcha-Lum, for stepping in and pouring so much love on me. Having you by my side in the last few months of my dissertation research was indeed favor from the throne of God.

I return the ultimate *"praise, and glory, and wisdom, and thanks, and honor, and power, and strength"* (*Revelation 7:12 a*) to my Lord and savior, Jesus Christ, who without whom I am nothing. It is You Lord that formed me in the belly of my mother and knew me before I was born and ordained me to be a success in this world (*Jeremiah 1:5*). I am eternally grateful.

Abstract

Evaluation of Brackish Water Desalination by Membrane Capacitive Deionization Systems: Performance Tradeoffs in Salt Removal, Hydraulic Recovery, Charge Efficiency, and Specific Energy Consumption

As potable water demand continues to exceed availability in several regions of the world, alternative water sources such as desalination and direct potable reuse have become of high importance in water sustainability discussions. The conventional desalination technologies include reverse osmosis (RO) and thermal distillation. Major barriers to the applicability of these technologies for desalination include inorganic scaling (RO) and high energy requirements respectively. This research provides an evaluation for the feasibility of Membrane Capacitive Deionization (MCDI), which is a technology gaining interest due to its theoretically low energy requirements for brackish water (less than 3 g/L) desalination. The motivation for this research is a deficiency in the literature of the parametric dependencies in MCDI, especially the effect of the operating hydraulic residence time (also known as the system detention time). The detention time is a parameter that allows for comparison between different MCDI devices across a range of sizes and flow rates. The first objective of this research was to perform a sensitivity analysis for different operating parameters on key desalination performance metrics in MCDI, as well as to analyze tradeoffs in operation at high hydraulic recovery. Furthermore, this research covered the development of a model based on equivalent electrical circuit to predict the performance of MCDI for desalination. The third objective was to evaluate the scale-up of high capacity aqueous processed electrodes for use in MCDI.

The experimental parametric analysis as discussed in this dissertation was performed with a commercial MCDI device and a laboratory fabricated MCDI unit. It was observed that operating

the MCDI device at higher detention times showed lower charge efficiency and resulted in higher specific energy consumption. The total cumulative salt removal was observed to increase with increasing detention time up to 60 s, beyond which there was marginal difference in salt removal but steady decline in charge efficiency. An increase in feed (sodium chloride) salinity from 1,302 mg/L to 5,271 mg/L for the same detention time also decreased the charge efficiency of the system from 74% to 50%, respectively. The Simplified Randles electrical circuit model that was developed in this research was able to accurately simulate the electrical current, charge efficiency, and product conductivity performance for detention time less than 60 s and cell voltage less than 1.2 V. The least root mean squared error (RMSE) analysis used for the model development was able to generate charge efficiency predictions within 3% of measured values for seventeen different experiments. The aqueous processed electrodes fabricated and tested in a laboratory-built reactor had a salt adsorption capacity of 0.41 meq/g, exceeding performance observed by collaborators at initial small-scale development. Overall, the findings of this research will help industries and municipalities identify the applicability and tradeoffs for the use of MCDI for desalination of brackish water.

Table of Contents

List of Tables

List of Figures

Abbreviations

AEM – Anion Exchange Membrane

CDI- Capacitive Deionization

CE – Charge Efficiency

CEM – Cation Exchange Membrane

DFM – Dispersed-Flow-Model

EDL – Electric Double Layer

EF – Equal-Flow

ERC - Engineering Research Center

GA – Glutaraldehyde

GCS – Gouy-Chapman Stern

IEM – Ion Exchange Membrane

KBH – Kay Bailey Hutchinson desalination plant (El Paso, TX)

LF – Low-Flow

MCDI – Membrane Capacitive Deionization

mD – modified-Donnan model

NEWT – Nanotechnology Enabled Water Treatment

NF – No Flow

NSEC – Normalized Specific Energy Consumption

PR – Polarity Reversal

PVA – Poly Vinyl Alcohol

RC – Resistor-Capacitor

RCR – Simplified Randles Circuit

RMSE – Root Mean Squared Error

RTD – Residence Time Distribution

SAC – Salt Absorption Capacitance

SC – Short-Circuit

SCADA – Supervisory Control and Data Acquisition

SEC – Specific Energy Consumption

TDS – Total Dissolved Solids

TIS – Tanks-in-Series

VBA – Visual Basic for Application

Mathematical Symbols

A: *An operational constant* (Ω)

Area: The total cross-sectional area of the flow channel (cm^2)

B: *An operational constant* (cm^{-1})

C: Capacitance (Farads)

C_{feed}: feed salt concentration (eq/L)

$C_{prod}(t)$: The salt concentration (eq/L) of the product at time, *t*

C_{Prod_t}: Concentration of product water with respect to time (meq/L)

E: Invested energy

$E\left(\frac{t}{\bar{t}}\right)$: Exit age distribution

F: Faraday's number (96485.3 C eq^{-1})

$F\left(\frac{t}{\bar{t}}\right)$: Cumulative distribution function

I: Electrical current measured (Amps or C/s)

$I(t)$: Current response in time, t (Amps or C/s)

i_1, i_2, i_3: Current response at constant voltage operation

$M_{electrode}$: Mass of the anode and cathode (g)

N: The number of tanks in series

$N_{desalted}$: Number of coulombs of salt removed

$N_{electric}$: Number of electrical coulombs invested

$P_{elec}(t)$: Invested electric power

Pe: Peclet number

$P_{hyd}(t)$: Hydraulic power (pumping power)

Q: Flow rate (L/s)

Q_{feed}: Feed flow rate

$Q_{product}$: Product phase flow rate

$r(t)$: Hydraulic Recovery at time, *t*

$R(t)$: Instantaneous conductivity reduction at time, *t*

R: Resistance (Ohms)

$Removal\ (t)$: The average conductivity reduction at any time during the adsorption phase

SAC: Salt Adsorption Capacity (meq/g)

SAC_f: Salt adsorption capacitance of charging phase (Farad)

$SEC(t)$: Specific Energy Consumption at time, *t*

t: Time

$\bar{t}$: The mean hydraulic detention time (s)

V: Volume of produced water

V: Applied voltage (Volts)

α: A constant based on the ratio of R_1 and R_2

$\eta_c(t)$: Charge efficiency

Θ: Dimensionless time

K_f: *C*onductivity of the feed solution

K_t: Conductivity during the product phase at time, *t*

$K_{(logmean)}$: Logarithmic mean of the feed conductivity (S/cm)

μ_s: Superficial velocity (cm/s)

τ: Detention time of MCDI reactor

General Introduction

Providing clean and affordable drinking water has become one of the most pressing challenges of the 21st century. This challenge is more prominent in developing countries of the world, as emphasized at the 2010 general assembly plenary of the United Nations (United Nations General Assembly 2010). Saline waters such as brackish water and sea water are alternative sources for water supply but require reduction of the salt content. The conventional technologies used for treatment of high salinity waters include reverse osmosis and thermal distillation (Elimelech and Phillip 2011). Inorganic scaling has been identified as a barrier that significantly hampers the performance of membrane desalination such as reverse osmosis (Quay et al. 2018; R. Zhang et al. 2016). Thermal desalination processes also have high energy requirements which limits their application for saline water desalination (Ghaffour et al. 2015; Ghaffour et al. 2013). Other desalination methods may be more economical or more effective and, therefore, more research is needed. This research helps to contribute to the knowledge of the feasibility of Capacitive Deionization (CDI) as an energy-efficient desalination technology (Anderson et al. 2010; Porada, Zhao et al. 2013).

CDI is a term used to define a range of technologies that use electrically charged porous electrodes for ion separation from saline water and subsequent release of these ions when the electrodes are discharged (M. Suss, Porada, Sun, Biesheuvel, Yoon and Presser 2015; Dykstra et al. 2016). CDI also promises to be an economical alternative for desalination of brackish water (Tang et al. 2017). Recently, several methods have been developed with deviations from the term "capacitive", but these technologies use the same concept of ion electrosorption and desorption using porous electrodes (Biesheuvel et al. 2017; Guyes et al. 2017; Yang et al. 2017). For instance, the addition of ion exchange membranes in front of porous carbon electrodes is known as

Membrane Capacitive Deionization (MCDI), and MCDI helps to overcome the adsorption of co-ions, that is, ions of same polarity as the electrode (Lee et al. 2006; Li and Zou 2011; Fritz et al. 2018). Ion exchange resins are also directly incorporated into the electrode or electrodes coated with ion selective coatings for higher efficiency (J. Kim and Choi 2010; Liu et al. 2014; Palakkal and Arges 2017; Jain et al. 2018; Zuo et al. 2018). This research ensures the use of metrics that allow for comparison with other CDI devices and with other desalination technologies. For CDI to become a standard desalination technology, CDI research must show comparable performance metrics with other desalination technologies and scalability from small laboratory scale to domestic, municipal, or industrial scale.

This dissertation is in collaboration with the National Science Foundation Nano-systems Engineering Research Center for Nanotechnology Enabled Water Treatment (NEWT EEC 1449500). The NEWT center works to identify and develop technologies that enhances provision of clean water anywhere in the world. MCDI has been identified by the NEWT center as a technology capable of tapping from unconventional water sources. This dissertation, therefore, helps to elucidate the feasibility of MCDI for high salinity water desalination. The dissertation is divided into three chapters covering experimental and model-based evaluation of brackish water desalination by membrane capacitive deionization (MCDI). The first chapter discusses a parametric analysis of MCDI with different key desalination performance metrics. The second chapter focuses on the development of a model for desalination performance prediction, while the third chapter covers the fabrication of an MCDI reactor incorporating the use of aqueous processed electrodes in a bench scale multicell set up.

Chapter 1 Parametric Analysis of Membrane Capacitive Deionization Performance for Synthetic and Real Brackish Water Desalination

Abstract

Membrane capacitive deionization (MCDI) is a desalination method that uses electrical voltage across two porous electrodes with ion exchange membranes (IEMs) to remove ions from saline water. The purpose of this research was to characterize the sensitivity of key MCDI performance metrics such as salinity removal, hydraulic recovery, and specific energy consumption to key operating parameters such as applied voltage, detention time and feed water salinity. Multiple experiments were performed with sodium chloride solutions in brackish water concentrations to identify optimum operating conditions. Experiments were then performed on real brackish water from El Paso Water's Kay Bailey Hutchinson desalination plant to demonstrate methods for achieving high hydraulic recovery. All experimental results and calculations used in the understanding of system performance were normalized to allow applicability by other researchers. The research findings showed that increasing MCDI reactor detention time yields higher salt removal but with a decline in charge efficiency for the system. An effective reactor detention time of 15 s to 60 s and an applied voltage of 1.2 V was selected for the 2,380 mg/L brackish water experiments. Results showed possibility of achieving water recovery ranges from 56% to 99% with a cumulative SEC range of 0.3 kWh/m^3 to 1.2 kWh/m^3. The maximum single-pass conductivity reduction was from 32.5% to 76.2%.

Keywords: Membrane Capacitive Deionization, Brackish Water, Charge Efficiency, Specific Energy Consumption, Hydraulic Recovery

1.1 Introduction

1.1.1 BACKGROUND

Several research groups have described effects of different operating conditions on the performance of CDI devices to generate optimum conditions for operation. Huyskens et al., (Huyskens et al. 2013) used a factorial design of experiments to screen desalination performance parameters for a CDI unit in their work and were able to achieve between 78 % to 93% water recovery. Their experiments were performed on a single cell CDI unit (with ion exchange membranes known as MCDI in literature) with sodium chloride solutions (500 – 1000 mg/L) but did not define their operational detention times. They operated the discharge or concentrate phase by using a no flow period and afterwards a purging period to achieve higher recovery (Huyskens et al. 2013). Parameter-based evaluation has also been done and with the use of genetic algorithms to optimize the performance of CDI systems or by combining CDI with other technologies (Saleem and Kim 2018; Saleem et al. 2017). Broséus et al., (Broséus et al. 2009) performed experiments to determine the feasibility of MCDI for desalination of water spiked with different sodium chloride, ammonium and nitrate concentrations (raw water total dissolved solids (TDS) concentration of 940 mg/L to 1,290 mg/L). Their tests showed water recovery rates ranging from 64 % to 96 % and achieving a treated effluent of 60 to 160 mg/L at 1.25 V constant voltage operation. The discharge phase was operated by reversing polarity for electrodes regeneration, followed by a purge phase (Broséus et al. 2009). Xu et al., (Xu et al. 2008) evaluated the ion selectivity and capability of treating brackish produced water from natural gas operations and reported hydraulic recoveries on the order of 25% to 33%. The chemistry of the water tested was mainly sodium chloride with other ions at relatively low concentrations (Xu et al. 2008). Yu et al. (2014) also conducted research on the application of CDI to improve the overall recovery of a wastewater treatment facility from 75% to 90%, treating RO concentrate water from a municipal waste water treatment plant (TDS

undefined). Han, Karthikeyan, & Gregory (2015) performed experiments with sodium chloride solutions and achieved a recovery up to 80%, by polarity reversal in the concentrate phase. Yao & Tang (2016) also explored the use of different desorption modes for their CDI system, treating sodium chloride (793 mg/L). Their conclusion was that optimizing flow rates in the desorption phase is needed for reduction of concentrate water volume, but then didn't state water recovery values. The challenge of waste or concentrate disposal is also of high impact in the feasibility for the use of desalination for high salinity water, especially in inland cases. Therefore, it is important to have technologies that can achieve high hydraulic recovery with sufficient ion removal for desired water quality goals (Greenlee et al. 2009)

Although research has been performed extensively on CDI for water desalination since its introduction in 1960 (Porada, Zhao et al. 2013), to our knowledge there has not been detailed parametric experimental analysis to show operational parameter effects over a wide range of conditions for brackish water desalination. Specifically, the reactor detention time has often been omitted in publication by many researchers, thus making it difficult to compare among CDI investigations and among other desalination technologies. It is also important to show operational parameter sensitivity analysis and high recovery possibilities with the more efficient MCDI and with multiple cells, as applied in real world systems. This is the motivation for evaluating the desalination performance of MCDI over a wide range of operating parameters and brackish feed water salinity, as well as the ability to achieve high hydraulic recovery with a brackish water source.

1.1.2 RESEARCH GOALS AND OBJECTIVES

There were two major objectives to be achieved with this research, and they are as follows. The first objective was to benchmark the performance of MCDI for desalination of brackish water. This was achieved by performing experiments for the desalination of varying brackish water (sodium chloride) solutions using a commercially available MCDI unit. The parameters used were calculated and reported in normalized units that allow for understanding the effects of scaling up to a larger scale operation. The second objective was to identify the operational conditions to achieve high recovery and explore the tradeoffs in product water quality and specific energy consumption (SEC). This is a unique research question being answered with this paper. The use of different operational modes helps in identifying combinations to achieve high recovery by reducing the fraction of water in the concentrate phase in comparison to the product phase.

1.2 Methodology

1.2.1 EXPERIMENTAL MCDI SYSTEM

A commercial Voltea VS1 MCDI module was purchased for this research, and a photo is shown in Figure 1.1 (a). The VS1 module has a stack of 17 cells with an octagonal cross-section. The hydraulic inlet port is connected to an annular manifold around the octagonal cross-section, and the feed flows in the negative radial direction and exits from the center of the octagonal cross-section, as shown in Figure 1.1 (b). A residence time distribution (RTD) analysis was performed on the MCDI reactor, and depending on flow rate, the system behaved as 7 – 12 tanks-in-series (TIS) or as a dispersed flow reactor with a dispersion number of 0.032 – 0.096 (Supplemental Information).

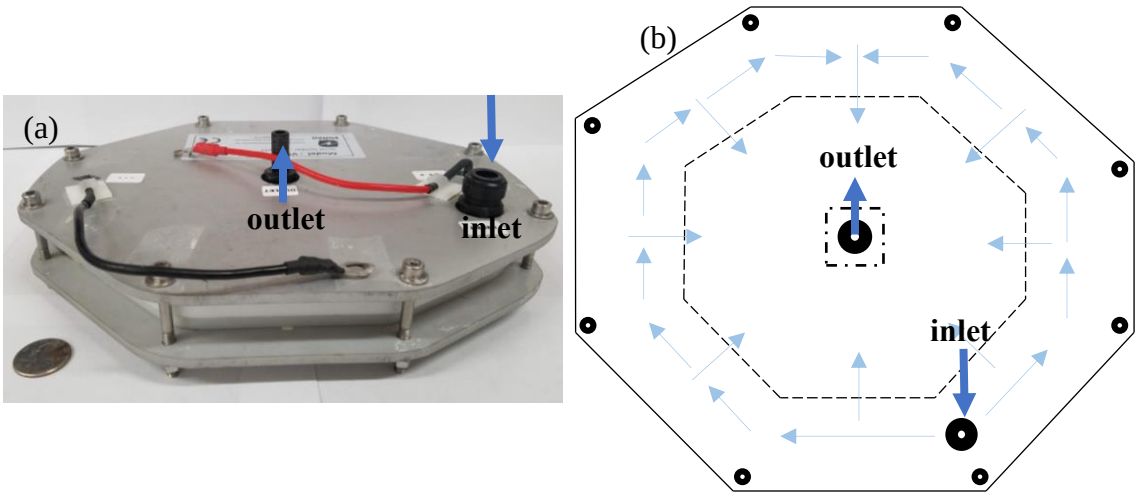

Figure 1.1: (a) Picture of Voltea VS1 Module and (b) Schematic of the Cross-Sectional Area for Voltea VS1 Module with flow path

National Instruments (NI) LabVIEW (2016) was used for creating a supervisory control and data acquisition (SCADA) system for MCDI operation. A BK Precision 9151 programmable DC power supply (20 V/27 A) with RS232 communication was used as the power supply unit for voltage applications. An NI multi-function I/O USB-6009 was used for monitoring the voltage across the terminals of the MCDI device. An NI cDAQ – 9174 USB chassis was used with NI 9264 (Voltage Output, -10 V to 10 V), NI 9265 (Current Output, 4 to 20 mA) and NI 9215 (Voltage Input, -10 V to 10 V) modules attached. A Hantek current clamp (CC-65) was connected to the NI 9215 cassette for monitoring the current in the adsorption and desorption phases. A programmable Masterflex pump drive (7528 - 10) with pump head (7518 - 00) was used for feeding water into the MCDI unit with Masterflex L/S 16 tubing. The Masterflex pump drive was controlled with a 4 mA to 20 mA signal from the NI 9265 module.

A Thermo Scientific Orion 5-star meter with pH probe (8107UWMMD) and conductivity probe (013005MD) was used for monitoring pH, oxidation reduction potential - ORP (mV), conductivity (mS/cm), and temperature (ºC) with RS232 to USB communication. The pH and conductivity probes were installed in flow through cells with an added volume of 10 mL and 5 mL

respectively. McMillan 111 and Omega FLR1000–11D flow meters were used to monitor the flow rate for flow ranges of 20 – 200 mL/min and 200 – 2000 mL/min respectively with the USB 6009 voltage analog input. Crydom D1D40 SPST relays were used for the automation of short-circuit and polarity reversal controls for the concentrate phase operation. The Crydom relays (normally open) were operated with voltage inputs (3.5 V – on, 1 V – off) from the NI 9264 module.

1.2.2 EXPERIMENTAL DESIGN

Experiments for MCDI unit benchmarking for brackish water desalination were performed with laboratory prepared synthetic sodium chloride (NaCl) solutions with a concentration range of 1,302 mg/L (22 mmol/L) to 5,721 mg/L (98 mmol/L) and conductivity of 2.5 to 10 mS/cm, respectively. Constant voltage operation was used for each experiment at a voltage range of 0.4 V to 1.2 V per cell. The detention time was controlled at 6 s to 180 s, corresponding to a flow rate of 320 mL/min to 11 mL/min, respectively. For the high recovery experiments, brackish water was obtained from Kay Bailey Hutchinson (KBH) desalination plant in El Paso, Texas. The average total dissolved solids (TDS) concentration and conductivity for this brackish water source were 2,380 mg/L and 4.66 mS/cm, respectively. The solutions and operational parameter ranges are listed in Table 1.1. All experiments were performed under constant voltage operation with complete electrode saturation before the desorption or concentrate phase (i.e., the voltage was not disengaged until the product conductivity returned to the original feed conductivity).

Table 1.1: Experimental design of brackish feed solutions and MCDI operational parameter ranges

Synthetic NaCl Solutions	
NaCl conductivity, K_0 (mS/cm) range	2.5 - 10
NaCl concentration (mg/L) range	1302 - 5271
Kay Bailey Hutchinson Desalination Plant Feed Water	
Total dissolved solids (TDS) (mg/L)	2380
Conductivity (mS/cm)	4.66
Range of Operating parameters	
Flow Rate (mL/min)	11 - 320
Detention time, τ (s)	180 - 6
Applied voltage (V)	0.4 - 1.2

The experiments were performed with the feed water fed through the MCDI unit for at least 30 minutes and until the influent and effluent conductivities were equal. The product (desalination) phase was initialized with the application of voltage. The product phase continued until the conductivity of the effluent from the MCDI unit equaled the feed conductivity (*i.e.*, maximum sorption and end of charging phase). The concentrate phase began by disengaging voltage application and short-circuiting the MCDI terminals (or applying a voltage with reversed polarity). The concentrate phase continued until all adsorbed ions were desorbed (complete desorption), *i.e.*, the point when the conductivity of the effluent equals the feed conductivity. The operating parameters and water quality for the 17 benchmark experiments are as shown in Table 1.2. These parameters were chosen based on brackish water concentration ranges. The usual voltage application range chosen does not exceed 1.2 V, since hydrolysis occurs at over 1.2 V (He et al. 2016).

Table 1.2: List of experiments performed for MCDI desalination of sodium chloride feed solution: applied voltage, detention time, and conductivity

Experiment Number	Voltage (Volts)	Detention time (s)	Feed Conductivity (mS/cm)
1	0.4	180	5
2	0.5	12	3
3	0.5	60	5
4	0.5	120	5
5	0.8	180	5
6	1.0	12	3
7	1.0	6	3
8	1.0	12	6
9	1.0	60	5
10	1.2	180	2.5
11	1.2	60	5
12	1.2	120	5
13	1.2	180	5
14	1.2	180	10
15	1.2	30	5
16	1.2	15	5
17	1.2	45	5

1.2.3 ANALYSIS OF SYSTEM PERFORMANCE

The performance of the MCDI system was determined by evaluating for salinity removal as conductivity reduction, hydraulic recovery, charge efficiency, and specific energy consumption. Each reported result is based on an average of a minimum of six adsorption/desorption cycles. A Visual Basic for Application (VBA) code was developed within Microsoft Excel for performing these calculations. Example conductivity data for four tests are shown in Figure 1.2.

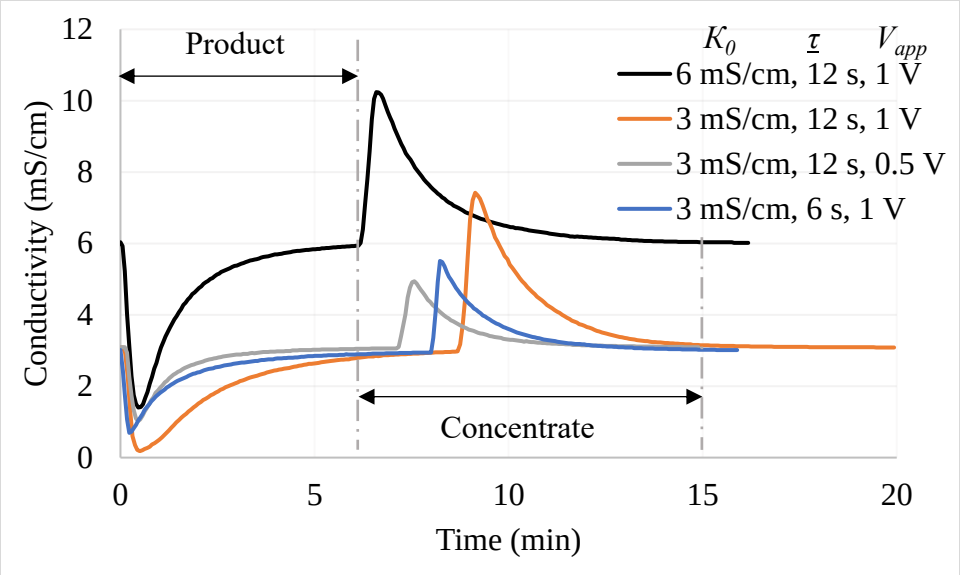

Figure 1.2: Raw conductivity data for four different experiments with different sodium chloride feed water concentrations (conductivity in mS/cm), operational detention time and applied voltage

1.2.4 CONDUCTIVITY REDUCTION (*R*)

The salt removal (*R*) is calculated based on the conductivity reduction (i.e., conductivity is proportional to total dissolved solids concentration). The conductivity reduction is calculated as:

Equation 1.1 $$R(t) = 1 - \frac{\mathrm{K}_t}{\mathrm{K}_f}$$

Equation 1.2 $$Removal\ (t) = \frac{\int_0^t R(t)dt}{\int_0^t dt}$$

where *R(t)* is the instantaneous conductivity reduction at any time (*t*) during the experiment, κ_t is the conductivity during the product phase at time *t*, and κ_f is the conductivity of the feed solution. *Removal(t)* is the average conductivity reduction at any time during the adsorption phase. Cumulative conductivity reduction is shown in Figure 1.3 (a) for test data in Figure 1.2. The maximum cumulative removal points are noted in Figure 1.3 (a). The dimensionless time (Θ) is calculated as:

Equation 1.3 $$\theta = \frac{t}{\tau}$$

where t is any time point during the test and τ is the MCDI reactor detention time.

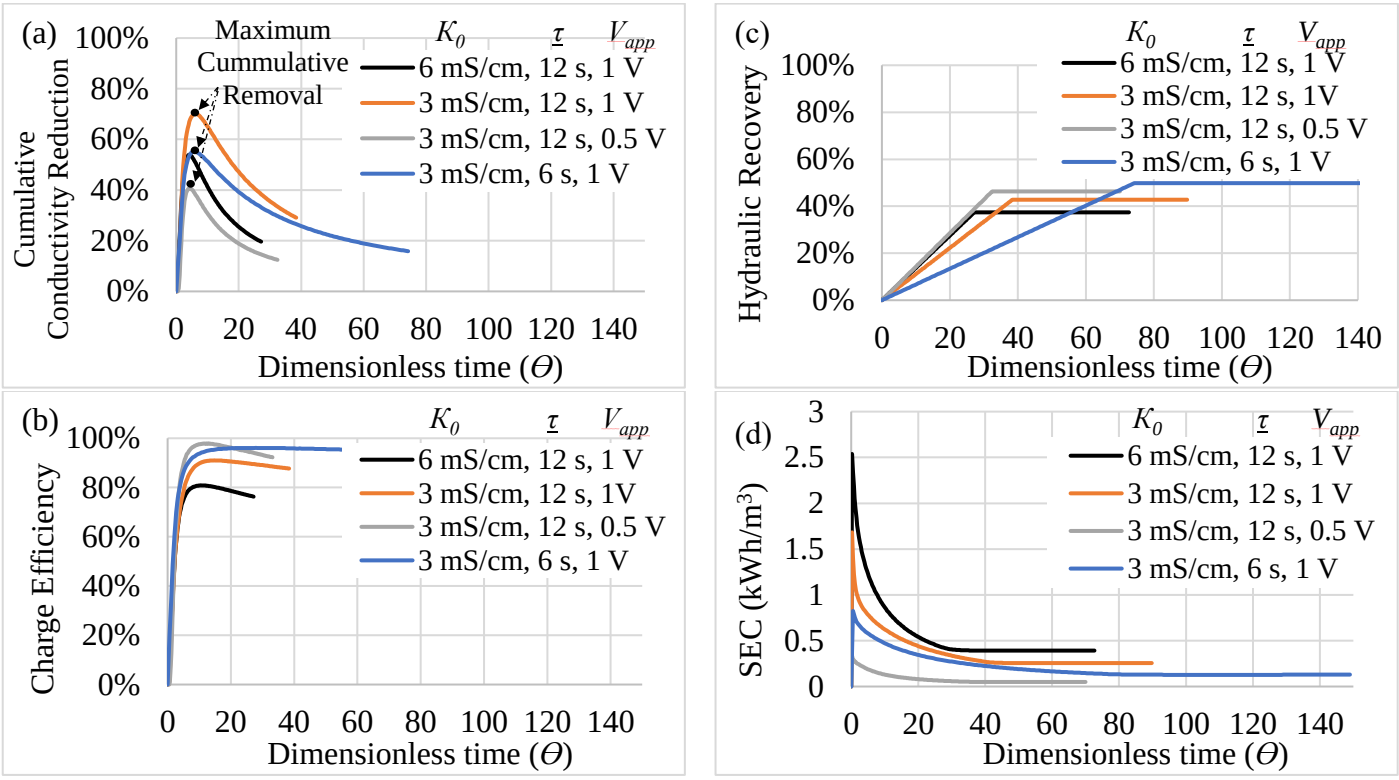

Figure 1.3: Desalination performance trends for four experiments with varying operating parameters for the Voltea VS1 MCDI device (a) Cumulative conductivity reduction (salt removal) (b) Charge efficiency (c) Hydraulic recovery (d) Specific energy consumption

1.2.5 CHARGE EFFICIENCY

Charge efficiency (η_c) describes the effectiveness of the invested electrical current in removal of ions from the feed solution (Zhao et al. 2009), and is calculated as:

Equation 1.4 $$\eta_c(t) = \frac{N_{desalted}}{N_{electric}} = \frac{\int_0^t F\left(C_{feed} - C_{prod}(t)\right)Q\,dt}{\int_0^t I\,dt}$$

where $N_{desalted}$ is the number of coulombs of salt removed, $N_{electric}$ is the number of electric coulombs invested, F is Faraday's number (96485.3 C eq^{-1}), C_{feed} is the salt concentration (eq/L)

of the feed, $C_{prod}(t)$ is the salt concentration (eq/L) of the product at time, t, Q is the flow rate (L/s), and I is the current measured (Amps or C/s). The charge efficiency is shown in Figure 1.3 (b) for example data shown in Figure 1.2.

1.2.6 HYDRAULIC RECOVERY

Hydraulic recovery (r) is the fraction of product water that is produced from the total volume of feed water.

Equation 1.5
$$r(t) = \frac{\int_0^t Q_{product}\, dt}{\int_0^{end\ of\ cycle} Q_{feed}\, dt}$$

where $Q_{product}$ is the flow rate during the product phase (adsorption), and Q_{feed} is the flow rate for each time step throughout the MCDI operation cycle. Recovery is shown in Figure 1.3 (c) for test data shown in Figure 1.2. A hydraulic recovery greater than 50 % is a result of a shorter concentrate phase than product phase with the same flow rate used for both phases.

1.2.7 SPECIFIC ENERGY CONSUMPTION (SEC)

The specific energy consumption (SEC) represents the energy consumption per unit volume of water that is produced (kWh/m^3) and is calculated as follows:

Equation 1.6
$$SEC(t) = \frac{E}{V} = \frac{\int_0^t \left(P_{elec}(t) + P_{hyd}(t)\right) dt}{\int_0^t Q\, dt}$$

where E is the energy invested, V is the volume of water produced (product phase), P_{elec} is the electric power invested into the MCDI for desalination, P_{hyd} is the hydraulic power (pumping power), and Q is the product flow rate at time *t,* during the experiment. Sample SEC calculations are shown in Figure 1.3 (d) for data shown in Figure 1.2.

1.2.8 CONCENTRATE PHASE OPERATION MODES

The operation modes in the concentrate phase are described in this section with notations assigned for each operation. The goal of the use of different operation modes was to identify a combination to achieve high hydraulic recovery.

SC: This indicates a short-circuit (SC) electrical operation during the concentrate phase.

PR: This designates an operation of polarity reversal (PR) during the concentrate phase.

EF: This is an equal-flow (EF) operation indicating the same flow rate of the product phase.

LF: This is a low-flow (LF) operation indicating a concentrate phase operation with reduced flow rate (higher detention time) compared to the product phase.

NF: This signifies a period of no-flow (NF) in the concentrate phase.

The above listed operation modes were combined in different forms to search for an optimum performance for high recovery combination.

1.3 Results and discussions

1.3.1 BENCHMARK ANALYSIS

Objective 1 involved the benchmark of membrane capacitive deionization and the determination of key performance parameters: salinity removal (R), hydraulic recovery (r), charge efficiency (η_c), and specific energy consumption (SEC). As shown in Figure 1.4 (b), a greater voltage application resulted in a greater end of cycle salinity removal for the same feed water salinity and detention time operation. Hence, the cumulative removal is dependent on the voltage applied for desalination and the hydraulic detention time of the system. The call-out numbers shown on the scatter plot in Figure 1.4 and Figure 1.5 represent the feed water conductivity for each experiment performed.

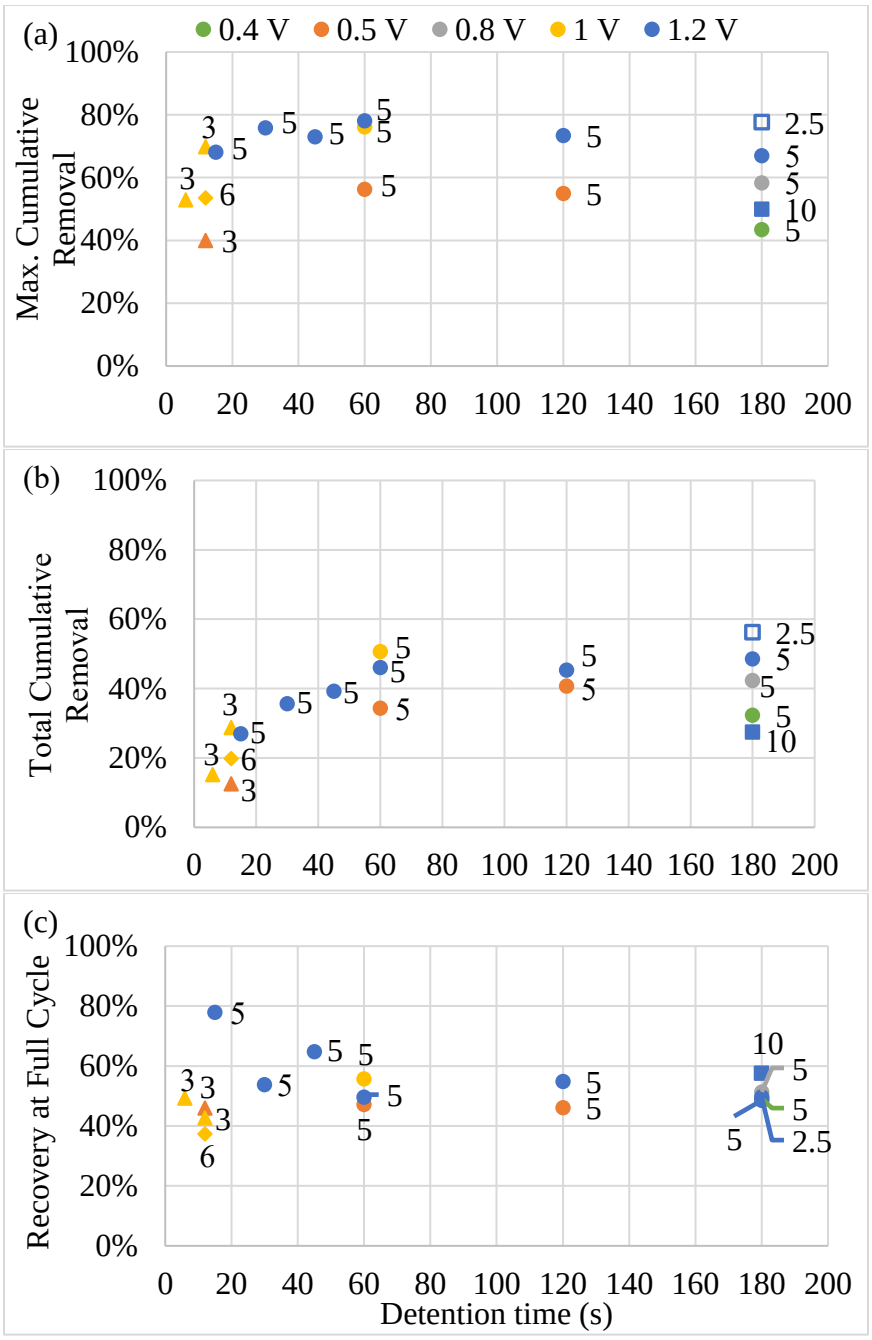

Figure 1.4: Results for experiments at different product phase applied voltage (marker color), flow detention times (x-axis) and feed water salinity (mS/cm, marker shapes and data callout numbers); (a) Maximum single-pass cumulative salinity removal (b) End of charging phase cumulative salinity removal (c) Hydraulic recovery at end of cycle

The total cumulative salt removal was observed to increase up to a detention time of 60 s, with marginal difference beyond the 60 s of operating detention time. The operating detention time analysis will mostly be different CDI or MCDI reactor electrode thickness, electrode density, ion

transport kinetics, and spacer to electrode thickness ratio. As shown in Chapter 3 here, a different reactor also showed very similar behavior.

As explained earlier, the hydraulic recovery of the system depends on the concentrate phase flow. All experiments except three shown in Figure 1.4 (c) were performed by the short-circuit (SC) and equal-flow (EF) modes for the concentrate phase. The experiments with 1.2 V applied for a feed conductivity of 5 mS/cm and product phase detention times of 15 s, 30 s, and 45 s were operated with concentrate phase detention times of eight, six, and three times the product phase, respectively.

As shown in Figure 1.5 (a) and (b), further experiments showed the charge efficiency (C.E.) varying based on the feed water salinity and detention time. Higher detention time operation showed less charge efficiency and requires further investigation into the reason for the inefficiencies observed at the higher detention time operation. Several researchers have attributed lower charge efficiencies to faradaic reactions in capacitive deionization (Lee et al. 2010; C. Zhang et al. 2018)

Operation with lower applied voltage resulted in a lower SEC for a given detention time and feed water salinity, as shown in Figure 1.5 (c) and (d). Operation at shorter detention time also resulted in a lower SEC for a given voltage and feed water salinity. Generally, higher detention time applications are not favorable with the current MCDI reactor design.

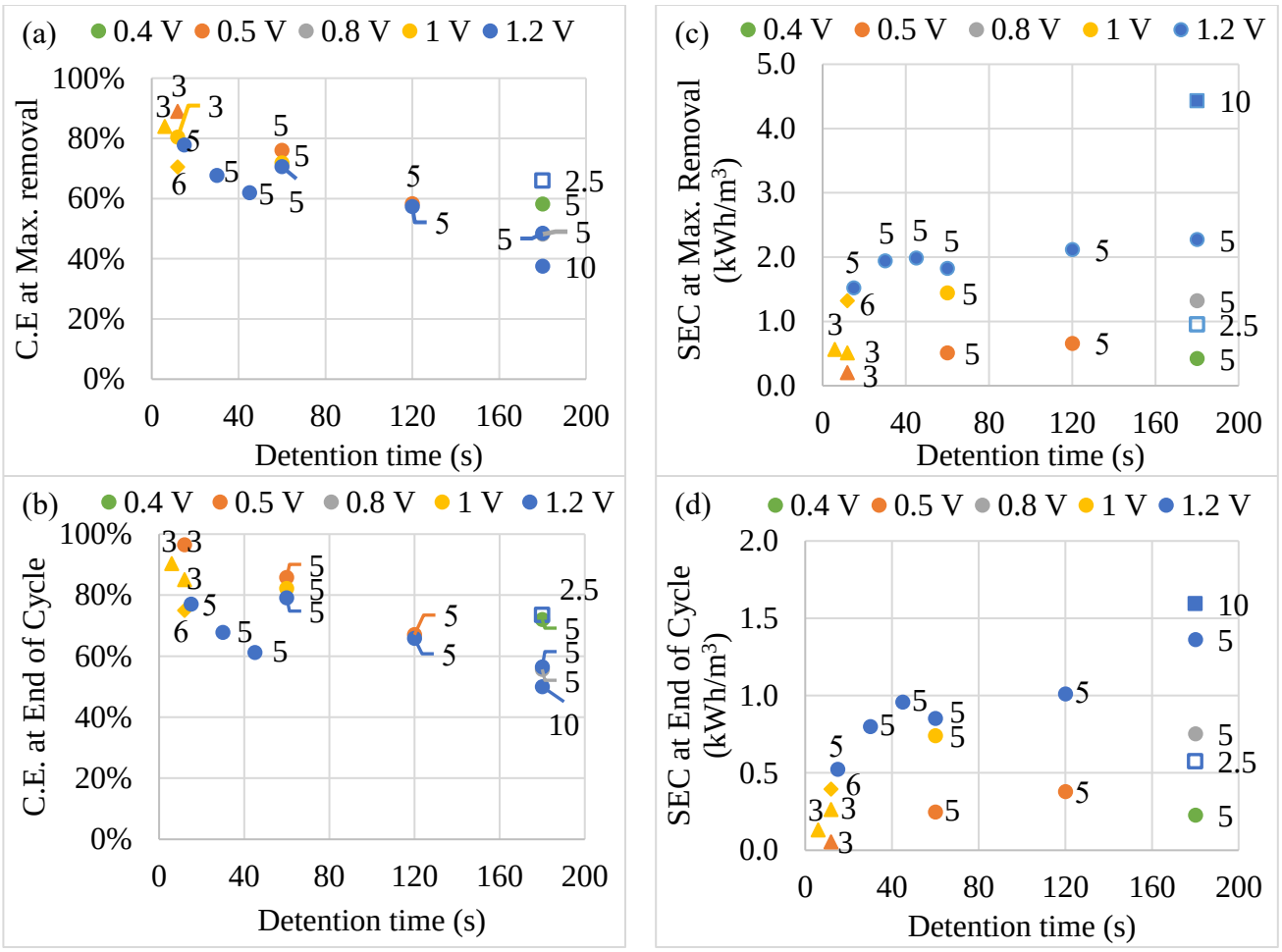

Figure 1.5: Results for experiments at different product phase voltage (marker color), detention times (x-axis) and feed water salinity (mS/cm, marker shapes and data callout numbers); Charge efficiency at (a) the point of maximum salinity removal, (b) end of cycle, and Specific Energy Consumption (SEC) at (c) maximum removal, and (d) end of cycle

1.3.2 ACHIEVING HIGH HYDRAULIC RECOVERY WITH REAL BRACKISH WATER

Experiments were performed with real brackish water to identify operation that results in high recovery by choosing different operation modes in the concentrate phase. Four experiments were performed on brackish feed water with an electrical conductivity of 4.72 mS/cm from the Kay Bailey Hutchinson (KBH) desalination plant in El Paso, Texas. Experiments were performed with product phase voltage of 1.2 V and product phase detention times of 12 s, 15 s, 45 s, and 60 s. The operation conditions and desalination performance for the four experiments are shown in

Table 1.3. The maximum and cumulative average conductivity reduction (salt removal) are shown in Figure 1.6 (a). The maximum conductivity reduction was achieved with a product detention time of 45 s.

Table 1.3: Operation conditions, Maximum Conductivity Reduction, Cumulative Conductivity Reduction, and Hydraulic Recovery for experiments with KBH desalination plant feed water

Product Phase Detention time (s)	Product Phase Flow Rate (mL/min)	Concentrate Phase Mode and duration (min)[1]	Conc. Flow Rate (mL/min)	Maximum Conductivity Reduction (%)	Total conductivity reduction (%)	Full Cycle Hydraulic Recovery
12	320	LF (7) PR (1) LF (3)	20[2]	32.5	10.1	99.95%
15	128	LF (74)	6.4	62.1	26.0	67%
45	43	LF (7) PR (1) LF (44)	6.4	76.2	41.6	75%
60	32	LF (7) NF (10) LF (70)	6.4	74.4	39.1	55.68%

The cumulative hydraulic recovery is shown in Figure 1.6 (b). The “LF-PR-LF” operation mode in the concentrate phase begins with low-flow (LF) mode for a fraction of the concentrate phase, followed by a short polarity reversal (PR) mode (-1.2 V), and then ends with LF mode. The “LF-NF-LF” mode begins with LF, followed by a now-flow (NF) mode and concluded by a LF mode. With a product phase detention time of 45 s, a recovery of 75% was achieved with the “LF-PR-LF" concentrate phase operation (more than one pass of MCDI treatment may be used to achieve desired product quality. The corresponding SEC (kWh/m^3) values for the four experiments are shown in Figure 1.6 (c). The SEC values at maximum sorption ranged from 0.3 to 1.2 kWh/m^3.

[1] Numbers in parenthesis represents duration for each mode of the concentrate phase operation
[2] Operation was at varying flow rates with an average of 20 mL/min

These experiments validate the possibility of achieving high recovery desalination with MCDI although it requires further tests to hone in on the optimum combinations.

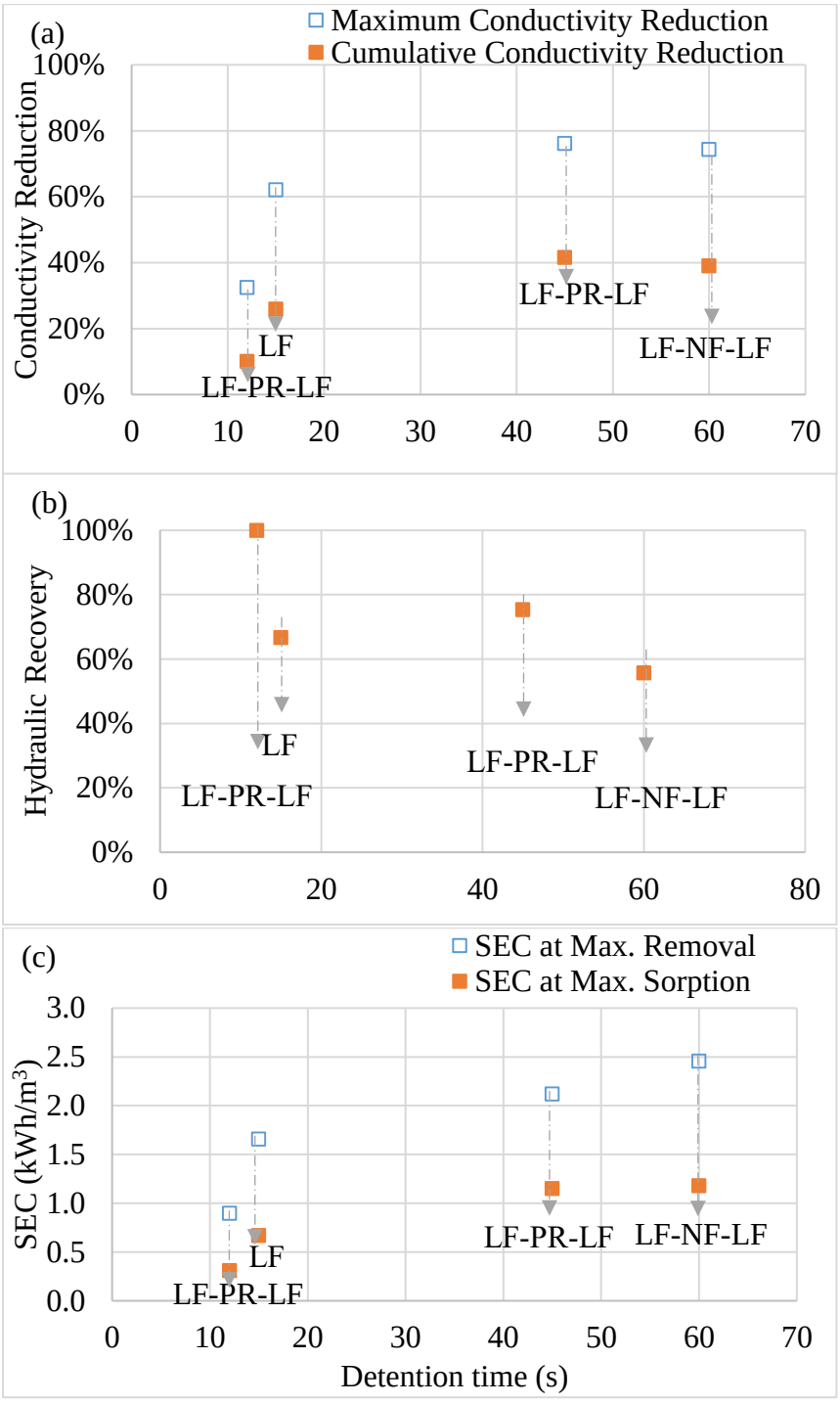

Figure 1.6: (a) Maximum and Cumulative Conductivity Reduction (b) Hydraulic recovery (c) Specific Energy Consumption (SEC) for KBH brackish water desalination by Voltea VS1 MCDI unit

1.4 Conclusions

This research evaluated the performance of a multicell commercial MCDI unit with ion exchange polymer coated electrodes for the treatment of brackish water. The main research objective was to establish a benchmark for MCDI performance and elucidate the effects of operating parameters of detention time, applied voltage, and feed water salinity on key desalination performance metrics of salinity removal, hydraulic recovery, charge efficiency and specific energy consumption. The importance of detention time for CDI research was established, as it helps to make meaningful comparisons within CDI research and with other desalination technologies. The charge efficiency in MCDI operations for the brackish water range tested has also helped to establish that in contrast to earlier conclusions in literature, higher feed water salinity has a negative effect on the charge efficiency. The SEC was mainly governed by the applied voltage and the resulting charge efficiency based on operation conditions, with higher voltage applications resulting in higher SEC values.

Furthermore, experiments were performed in the observed optimum operation conditions with real brackish water to establish a methodology for achieving high hydraulic recovery with minimal extra energy investment. The applied voltage for the real brackish water experiment was set at 1.2 V, and product phase detention times for the tests were 12 s, 15 s, 45 s, and 60 s. Different operation modes were used for the concentrate phase to identify a combination that gives the highest recovery. The concentrate phase operation of “LF-PR-LF” was determined to be the combination that gives the highest recovery. Hydraulic recovery greater than 75 % was achieved by the “LF-PR-LF” mode operating with a substantially lower flow rate during the concentrate phase. For the KBH brackish water treated at 45 s of detention time, a recovery of 75% was achieved with a single pass conductivity reduction of 42 %.

Chapter 2. Simplified Randles Circuit Model for Desalination Performance Prediction of Multicell Membrane Capacitive Deionization (MCDI) Systems

Abstract

Membrane Capacitive deionization (MCDI) is a desalination technology operating by the application of electrical voltage across porous electrodes with ion exchange membranes for removal of charged ions from water. The purpose of this research was to develop a mathematical model based on a Simplified Randles circuit to predict the desalination performance of an MCDI device used in treatment of water with brackish concentrations. Model development was performed after characterizing the relationships of the different MCDI systems metrics such as salinity removal, charge efficiency, hydraulic recovery, and specific energy consumption to different system operating parameters. The electrical current response for the multicell MCDI device was then modeled as a function of solution resistance, and the electric double layer capacitance of the MCDI device. The Simplified Randles Circuit (RCR) model was explored for constant voltage operation of MCDI. The RCR model varying resistance with effluent conductivity showed better performance with lower root mean squared error (RMSE). The current density predictions by the RCR model was suitable for operations at shorter detention times (6 s to 60 s).

Keywords**:** Capacitive Deionization, Simplified Randles Circuit, Membrane, Specific energy consumption, Brackish water

2.1 Introduction

2.1.1 BACKGROUND

Capacitive deionization CDI is a water desalination technology with promising energy efficiency for desalinating water with low ionic content, as in brackish water, and with the capability of energy recovery (Tang et al. 2016; Długołęcki and van der Wal 2013; Porada, Borchardt et al. 2013; M. E. Suss et al. 2012). CDI has been combined with ion exchange membranes, a configuration referred to as membrane capacitive deionization (MCDI) (Jain et al. 2018; Biesheuvel and Van der Wal 2010; Li and Zou 2011). MCDI can also be used to selectively remove different ions or compounds from a mixture. This selective separation capability is also an advantage over reverse osmosis and makes MCDI valuable for water treatment in the mining industry and in hospitals (Zhao et al. 2009; Y. Kim and Choi 2010; Yan et al. 2018).

For MCDI (used in this research for its higher efficiency for desalination) to become more competitive for water desalination, there is a need for the development of predictive models based on simple characteristics of the MCDI devices (M. Suss, Porada, Sun, Biesheuvel, Yoon and Presser 2015). The prediction model should help determine based on these characteristics of the MCDI device and the operation parameters employed, the MCDI performance in terms of desalination degree or salt removal, hydraulic recovery, and energy consumption.

Electrode materials in CDI are usually fabricated from porous activated carbon with high internal specific surface area. Experimental data have been used to develop and validate models for the double-layer structure of porous materials. There have been several studies to model the electric double layer (EDL) of CDI devices, most commonly by the Gouy-Chapman-Stern (GCS) and modified-Donnan (mD) EDL models (Johnson and Newman 1971; Guyes et al. 2017; Biesheuvel et al. 2011; Saleem and Kim 2018; Hemmatifar et al. 2015). The GCS model is a theoretical model that suggests that a high Stern layer capacity is beneficial for high salt adsorption.

Zhao et al (2009) used the equilibrium salt adsorption and electrode charge as input parameters for developing an electro-kinetic CDI process model based on GCS double layer model and further described by the equilibrium Poisson-Boltzmann equation. The Nerst-Planck equation has also been used for describing the transport of ions through electrodes or through ion-exchange membranes used in MCDI (Szymczyk et al. 2009). More recently models have been developed with device specific parameters of system volume, flow rate, and inlet water quality (Mutha et al. 2018). The complexity of these models has limited there application especially for real world systems.

Another approach to the modeling of CDI devices is the use of electrical circuit models such as the RC circuit model (Black and Andreas 2010). Qu et al. (2016) used first order analysis of energy dissipation by an RC circuit model to elucidate the energy consumption associated with the charging and discharging of a flow through CDI reactor. Qu et al. (2016) showed that the RC circuit model does not capture losses and inefficiencies such as reactions occurring on the electrode surface. They further described the resistive and capacitive components in CDI by the transmission line (TL) model. The TL model which is built upon constant salt concentration theories has also been discussed to have limitations for technologies with changing electrolyte concentration such as MCDI (Mirzadeh et al. 2014; M. E. Suss et al. 2012). Tang, He, Zhang, & Waite (2017) also used a circuit model based on different resistances of a commercial MCDI unit to characterize the voltage variation in the adsorption and desorption steps of their CDI operation. The preceding models discussed have helped in the understanding of CDI and MCDI performance mostly for salt removal (theoretical models) and for energy consumption. This research improves on the RC circuit model for the prediction of the current density response at different operation conditions. To our knowledge, no one has used an electric circuit model to effectively predict the desalination

performance of salt removal based on the current density for MCDI and the system charge efficiency.

2.1.2 GOALS AND OBJECTIVES

This research introduced and made use of the Simplified Randles Circuit Model based on simple characteristics of the MCDI devices to closely predict the MCDI devices desalination performance, and charge efficiency. The novelty of this research is in the application of the Simplified Randles Circuit for the prediction of the electrical current and the charge efficiency of the MCDI system in the charging phase. Furthermore, as never shown before, the effective current was used to predict salt removal and effluent conductivity with application to different feed salinities. Considering that water quality differs from one location to the other, a model with simplified characteristics of the MCDI device is highly beneficial for MCDI applications.

The first objective was to develop a Simplified Randles electrical circuit model to simulate the electrical current and charge efficiency of an MCDI device, and the second objective was to simulate salt removal based on the predicted current.

2.2 Methodology

2.2.1 EXPERIMENTAL MCDI SYSTEM

The supervisory control and data acquisition (SCADA) system used for the experiments reported here is as explained in Chapter 1. Experiments were performed on the Voltea VS1 MCDI module and were used to develop the equivalent circuit models.

2.2.2 EXPERIMENTAL DESIGN

Experiments were initially performed on the commercial MCDI unit as described in Chapter 1. The experiments were performed at constant voltage application and by allowing for full adsorption capacity before desorption of the electrodes (*i.e.* charging phase duration was ended when the effluent conductivity equaled the feed conductivity). The operating parameters of applied voltage, detention time, and sodium chloride feed water conductivity for the experiments used in this chapter are listed in Table 2.1.

Table 2.1: List of experiments discussed for MCDI model with applied voltage, detention time, and sodium chloride feed solution conductivity

Experiment Number	Voltage (Volts)	Detention time (s)	Feed Conductivity (mS/cm)
1	1.2	15	5
2	1.2	60	5
3	1.0	12	3
4	1.0	60	5
5	0.5	12	3
6	0.5	60	5

2.2.3 ANALYSIS AND CALCULATIONS FOR DETERMINING SYSTEM PERFORMANCE

Calculations for evaluating the system performance in terms of salinity removal, hydraulic recovery, charge efficiency, and specific energy consumption were performed as described in Chapter 1. In addition to the earlier stated calculations, the adsorption or charging phase salt adsorption capacitance (SAC_f) for each experiment was calculated using the equation below. This salt adsorption capacitance was then normalized by the MCDI reactor total surface area.

Equation 2.1
$$\mathrm{SAC_f}\ (Farad) = \int_0^t \frac{F\left(C_{feed} - C_{prod}(t)\right) Q dt}{V}$$

where F is Faraday's number (96485.3 C eq^{-1}), C_{feed} is the salt concentration (eq/L) of the feed, $C_{prod}(t)$ is the salt concentration (eq/L) of the product at time, t (s), Q is the flow rate (L/s), and V is the applied voltage for the respective experiment. The MCDI system product phase superficial velocity was also determined as a function of the system flow path using the following equation.

Equation 2.2
$$\mu_s = \frac{Q}{Area}$$

where μ_s is the superficial velocity (cm/s), Q is the volume flow rate of the reactor (cm^3/s), and *Area* is the total cross-sectional area of the flow channel (cm^2).

2.2.4 MODEL DEVELOPMENT

A resistor-capacitor (RC) circuit model (Figure 2.1) was used as the first step to simulate the electrical current with respect to time for the MCDI units during the charging phase.

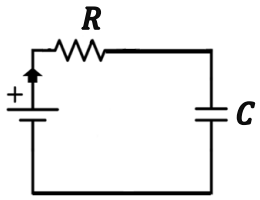

Figure 2.1: RC Circuit diagram

The RC circuit consists of a resistor and a capacitor in series with a power source. For constant voltage application to a CDI reactor, the current response is defined by the following equation (Qu et al. 2016).

Equation 2.3 $$I(t) = \frac{V}{R}\, e^{-\frac{t}{RC}}$$

where *V* is the voltage applied in Volts, *R* is the resistance in Ohms, and *C* is the capacitance in Farads. The RC circuit model does not effectively model the losses that occur in MCDI operation but has been used for energy consumption estimation (Qu et al. 2016).

The Simplified Randles Circuit (RCR) model as shown in Figure 2.2 was developed and used for modeling the current in the adsorption phase.

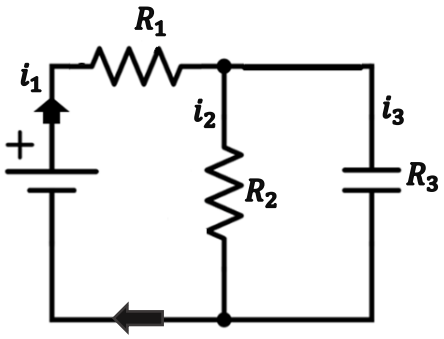

Figure 2.2: Simplified Randles Circuit (RCR) diagram

The current through Resistor 1 (R_1), i_1, which is the location at which experimental current is being observed, must equal the sum of the current through the capacitor, i_3, (*i.e.*, effective desalination) and the loss, i_2, through the added parallel resistor (R_2). The equations for the current response at

constant voltage operation with respect to time using the RCR circuit for i_1, i_2, and i_3 are derived and shown below.

Equation 2.4
$$i_1 = i_2 + i_3$$

Equation 2.5
$$i_2(t) = \frac{V}{\alpha R_2}\left(1 - \exp\left(\frac{-\alpha t}{R_1 C}\right)\right)$$

Equation 2.6
$$i_3(t) = \frac{V}{R_1}\exp\left(\frac{-\alpha t}{R_1 C}\right)$$

where C is the capacitance. V is the constant voltage being applied, t is the time, and α is a constant based on the ratio of R_1 and R_2 as shown below.

Equation 2.7
$$\alpha = 1 + \frac{R_1}{R_2}$$

The first step of the model development involved the use of empirical mathematical solutions to predict the current response. An empirical RC circuit model was made using the Generalized Reduced Gradient algorithm in the solver add in tool of Microsoft Excel. The least root mean square error (RMSE) regression model for predicting the current density generates a local optimum solution for fixed objective variables of Resistance, R (ohms), and Capacitance, C (Farads) for the RC circuit. An empirical RCR model was then developed to compare the performance to the RC circuit model using the root mean square error (RMSE). The empirical RCR model generates a local optimum for constant values of R_1, R_2 and C. Furthermore, a third model was developed based on the empirical RCR model but with R_1 varying with respect to the

conductivity of the solution in the system and a fixed objective variable for *C.* For this third model, the values of R_1 (ohms) with respect to time *t* were calculated as follows:

Equation 2.8 $$R_1(t) = A + \frac{B}{\mathrm{K}_{(logmean)}}$$

where *A* (Ω), and *B* (cm^{-1}) are constants based on respective MCDI system characteristics and operational conditions. $\mathrm{K}_{(logmean)}$ is the logarithmic mean of the feed conductivity (S/cm) and the product water conductivity (S/cm) (arithmetic mean is used when the feed conductivity is the same as the product conductivity).

The RCR models were subject to the following constraints:

At time *t* = 0, the value of R_1 was observed to be approximately constant across (*i.e.* independent of any experimental conditions) all 17 experiments listed in Chapter 1 with a value of 0.0583 Ω within a coefficient of variation of 5.4 %.

Hence at *t* = 0 $$R_1 = \frac{V}{i_1} \approx \frac{V}{i_3}$$

and R_2 is set based on the end of charging phase total resistance

so that $$R_2 = \frac{V}{i_{1_{at\ end\ of\ charging}}} - R_1$$

The charge efficiency at the end of the charging phase for the two RCR models was calculated by the following equation.

Equation 2.9 $$C.E = 1 - \frac{\Sigma\left[\left(\frac{i_2(t+1)+ i_2(t)}{2}\right)\Delta t\right]}{\Sigma\left[\left(\frac{i_1(t+1)+ i_1(t)}{2}\right)\Delta t\right]}$$

The current response i_3, which is the effective current resulting in salt removal was integrated to calculate coulombs of salt removed for the monovalent salt (sodium chloride) solutions used in

this research. The integration was performed using the difference in each time step between the feed water concentration and the number of effective electric coulombs invested per time step. A discretized residence time analysis was also employed for the operation detention time being modeled. The modeled concentration as a function of the current i_3, is calculated with the following equation.

Equation 2.10 $$C_{Prod_t} = C_{feed} - \frac{\sum_{k=1}^{\infty}[(F_{t-k} - F_{t-(k+1)}) \times (\frac{i_{3t-k} + i_{3t-(k+1)}}{2})]}{F \times Q}$$

where C_{Prod_t} is the product water concentration (meq/L) with respect to time, t (s), C_{feed} is the concentration of the feed solution (meq/L), F is the Faraday constant (96485.3 C/eq), and Q is the flow rate (L/s).

2.3 Results and discussions

2.3.1 Experiment Results

The salt adsorption capacitance (SAC_f) normalized by the total MCDI electrode surface area for six experiments of the total 17 from Chapter 1 with the Voltea VS1 MCDI Module are plotted against the superficial velocity as shown in Figure 2.3. The six experiments shown were at 1.2 V constant voltage operation and 5 mS/cm sodium chloride feed solution with varying operating detention times. This is to show the effect of system operation superficial velocity based on the operation detention time on the SAC_f measured. Operating the MCDI system at higher superficial velocities correlating to lower detention times resulted in higher SAC_f and higher charge efficiencies as earlier explained in Chapter 1. This detention time effect was further observed to be of high significance in the modeling of the system performance as explained with the equivalent circuit model.

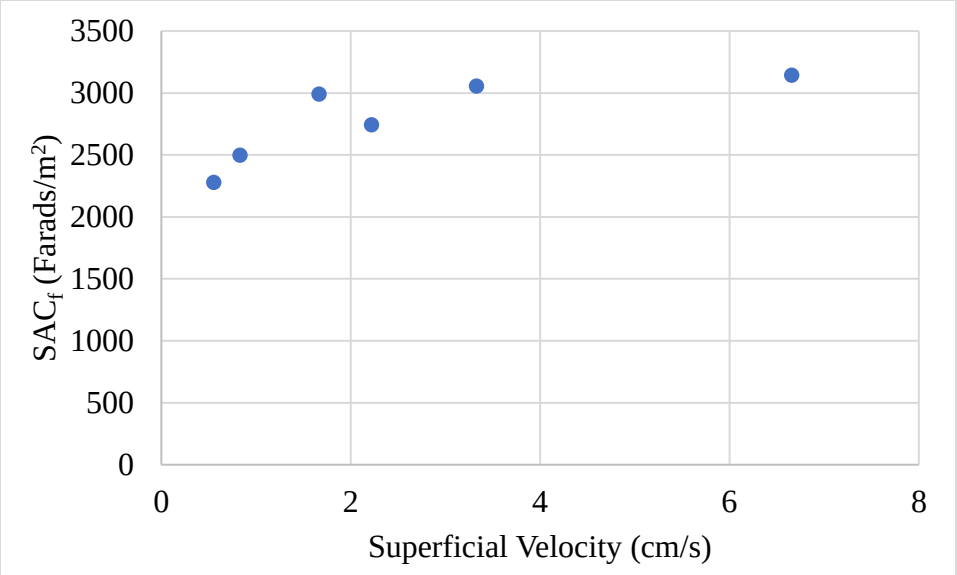

Figure 2.3: Calculated salt adsorption capacitance (Farad/m^2) for the Voltea VS1 MCDI unit with respect to superficial velocity, for varying operating parameters of applied voltage, detention time and feed water conductivity

2.3.2 ELECTRICAL CIRCUIT MODELS

The empirical models for the current response using the RC and Simplified Randles Circuit (RCR) model was developed for an experiment with an applied voltage of 1 V, 12 s of detention time, and 6 mS/cm of sodium chloride feed water. A least square error regression analysis was performed to determine the resistance and capacitance for each electric circuit model. The current density response in the adsorption phase for each model is as shown in Figure 2.4 (a). The current density for this unit was calculated based on a single cell electrode surface area of 213 cm^2 and 17 MCDI cells. The summary of the measured value and different model predictions for resistance, capacitance and charge efficiency, and the RMSE for the current density by each model are shown in Table 2.2. The experimentally measured capacitance is the salt adsorption capacitance at the end of the adsorption phase for the experiment in question (Farads/m^2). In comparison to the experimental result, the RCR with varying resistances was the best performing model based on the room mean squared error (RMSE) analysis. This model was then selected and used to predict the product phase conductivity from the effective current (i_3), through the capacitor. The conductivity

prediction is shown in Figure 2.4 (b) with discretized residence time distribution applied for the reactor.

Table 2.2: Comparison of experimentally measured parameters to model predicted values for a 1 V, 12 s, and 6 mS/cm experiment with the Voltea VS1 MCDI unit, and the Root Mean Squared Error (RMSE) for current density prediction by each model

Parameter	Experimentally Measured	Empirical RC	Empirical RCR (constant)	Empirical RCR, Varying R_1 with conductivity
Capacitance (Farads)	950	1191	1011	1097
R (Ohms)	-	0.061	-	-
R_1 (Ohms)	-	-	0.06	0.05 - 0.08
R_2 (Ohms)	-	-	0.85	0.81 - 0.88
Charge Efficiency (%)	75	-	68	76
RMSE (A/m^2)	-	0.80	0.50	0.28

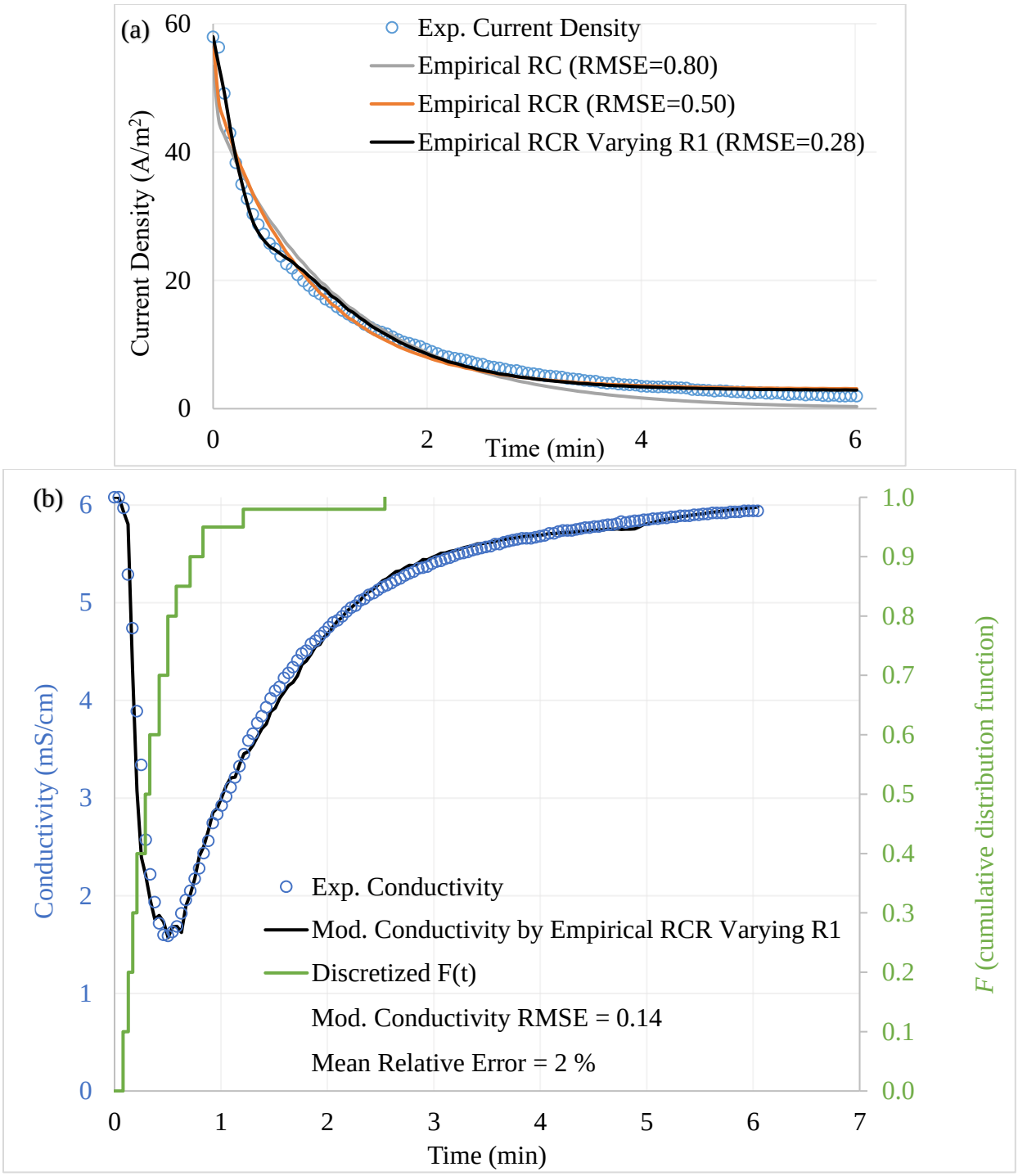

Figure 2.4: (a) Current response model in the adsorption phase for a 1 V, 15 s, and 5 mS/cm sodium chloride experiment with Voltea VS1 MCDI unit. Model by an Empirical RC circuit, Empirical RCR circuit, and Empirical RCR with varying resistances (b) Experimental and predicted product phase conductivity from modeled current response and discretized F(t) (secondary axis) for conductivity calculation from modeled i_3.

The next phase was the testing of the developed model for other experiments with the Voltea VS1 MCDI module. The current density prediction based on the RCR with varying R_1 (RCR) model is shown in Figure 2.5 (a) to (f) for six experiments from Chapter 1 with varying operations of applied voltage, detention time, and feed water conductivity.

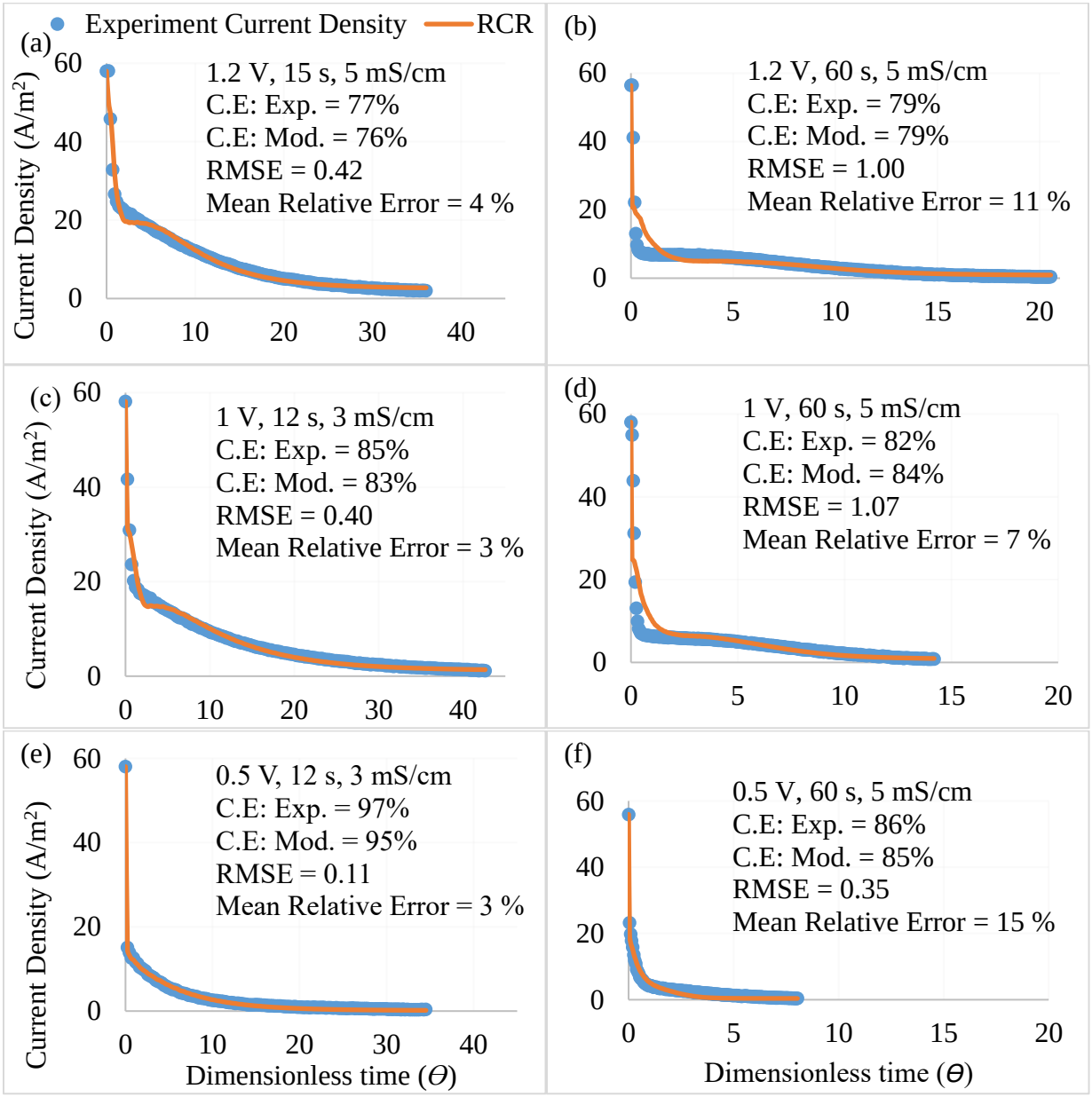

Figure 2.5: Measured and predicted current densities, and charge efficiencies for six experiments at varying operating conditions for desalination of brackish feed water by the Voltea VS1 Module MCDI unit

For the six experiments shown in Figure 2.4, the fitting parameter values of A (Ω) and B (cm^{-1}) of Equation 2.8 as well as capacitance (C) are listed in Table 2.3.

Table 2.3: Fitting parameter values A (Ω), B (cm^{-1}), Capacitance per unit area ($Farads/m^2$), and measured salt adsorption capacitance SAC_f per unit area for six experiments with the Voltea VS1 MCDI unit

Experiment[3]	A (Ω)	B (cm^{-1})	Model Salt Adsorption Capacitance ($Farads/m^2$)	Measured SAC_f/m^2 ($Farads/m^2$)	RMSE (A/m^2)
1.2, 15, 5	0.012	0.0064	3978	3143	0.42
1.2, 60, 5	0.0009	0.0187	4016	2991	1.00
1, 12, 3	0.055	0.0025	3174	2768	0.40
1, 60, 5	0	0.0126	4074	2900	1.07
0.5, 12, 3	0.0916	0.0005	2005	2058	0.11
0.5, 60, 5	0.0001	0.0080	1707	2235	0.35

The current response model showed the behavior of the MCDI unit based on different operation conditions. The lower detention time operations began exponential decay at a much higher current density than the higher detention time operations, which is a behavior closer to the RC Circuit model. Longer charging times were also seen for longer detention time operations at higher voltage applications. Overall, the RCR model was able to generate close predictions for the charge efficiency measured with less than 3% difference for the six experiments shown. The A (Ω) and B (cm^{-1}) parameter constant for this device was determined to range from 0 to 0.11 and 0 to 0.02, respectively. Better model fits (*i.e.* lower RMSE values) were correlated with shorter detention times and lower voltage applied as shown in the RMSE values displayed on the figures. Further information about the models and a summary table for the model predictions, experimental values, and RMSE for all 17 experiments from Chapter 1 are shown in Appendix B.

[3] Applied Voltage (V), Detention time (s), Feed water conductivity (mS/cm)

2.4 Conclusions

In this research, three different model types based on electric circuits were tested to predict the performance of an MCDI device based on operational characteristics and device characteristics. The Simplified Randles circuit (RCR) model was developed and used to predict the performance of a Voltea VS1 MCDI device at different operation conditions. The RCR model with varying resistor R_1 with conductivity was found to be more accurate (*i.e.* lower RMSE) than the Empirical RC circuit or the Empirical RCR circuit models. The RCR model with varying R_1 was also used to calculate the charge efficiency and effluent conductivity. The model prediction was more accurate for lower detention time operations, which are preferred as in real world systems due to the higher charge efficiency and smaller footprint. This model also presents a research question for the development of a model based on the RCR model for multicomponent water types. This research has shown the usefulness of an equivalent circuit in predicting the current response for an MCDI device and the corresponding conversion of the current response to the effluent conductivity.

Chapter 3. Scale-up of high capacity aqueous processed electrodes for membrane capacitive deionization

3.1 Introduction

3.1.1 BACKGROUND

Membrane capacitive deionization (MCDI) is a desalination technology rapidly gaining interest from researchers due to its lower energy requirements for low salinity water (<3 g/L) desalination (Porada et al. 2013; Wang et al. 2018; J. Zhang et al. 2017). MCDI uses porous electrodes with ion exchange membranes placed in front of the electrodes to remove ions from water when an electrical charge is applied. The ion exchange membrane helps prevent the transport of co-ions into electrodes with the same polarity (Biesheuvel and Van der Wal 2010). The use of organic solvents in the fabrication of electrodes for CDI has been found to be critical in the environmental impact assessment of the technology (T. Yu et al. 2016). Jain et al. (2018) established the need for alternative methods for electrode fabrication while reducing dependence on the use of organic solvents. The salt adsorption capacity and charge efficiency for MCDI has also been established as highly significant for the technology to gain applicability for desalination (J. S. Kim et al. 2016; Omosebi et al. 2015; Bian et al. 2015).

As in most developing water treatment technologies, the ability to scale up from small scale to large scale and reproducing the same performance achieved at small scale is very important (Xu et al. 2008; Subramani and Jacangelo 2015; Lai et al. 2018). Jain et al. (2018) developed a scalable completely aqueous processed electrode for capacitive deionization (CDI). The performance of these electrodes at small scale (single cell 10 cm x 1cm) when paired with ion exchange membranes exhibit salt adsorption capacity up to 0.308 meq/g (Jain et al., 2018). In this research, we showed the scale up of the aqueous processed electrodes with the addition of ion exchange

membranes in a bench scale multicell MCDI system for the treatment of synthetic brackish water. The performance of the MCDI reactor with a single electrode size of 20 cm x 9 cm (total and effective electrode size) and with up to 16 MCDI cells was evaluated at different operating conditions. The effect of scaling up of the aqueous processed electrodes is demonstrated using key desalination performance metrics of conductivity reduction, charge efficiency, hydraulic recovery, and specific energy consumption.

3.1.2 GOALS AND OBJECTIVES

The goal of this research was to evaluate the performance of aqueous processed electrodes at bench scale for brackish water desalination. The first objective was to fabricate a plate and frame multicell MCDI reactor. Secondly, the performance of the aqueous processed electrodes for MCDI was established with experiments at different number of cells and varying operating parameters. The performance was also compared to the performance of the commercial MCDI reactor tested in Chapter 1. All comparisons were made based on key desalination parameters of conductivity reduction (salt removal), charge efficiency, hydraulic recovery, and specific energy consumption.

3.2 Methodology

3.2.1 AQUEOUS PROCESSED ELECTRODES FOR MCDI

The aqueous processed electrodes were made at larger sizes (20 cm x 9 cm) in the laboratory using CEP21K powdered activated carbon (PAC, surface area of 2100 m^2/g) from Power Carbon Technology Co., Ltd., Republic of Korea. The 2010A-00539100 graphite sheet used as the current collector was obtained from Mineral Seal Corporation, USA with a thickness of 0.005-in (0.13 mm). The electrodes were made using water-soluble poly vinyl alcohol (PVA, 89,000 – 98,000 g/mol, >99% hydrolyzed) as binder and glutaraldehyde (GA, 25% in water) as the crosslinker. A 6% by weight PVA solution was first prepared by mixing in deionized water at

90 °C for 4 h. GA solution was then added at ambient temperature at 5% mol/mol and mixed for 1 hr. The PAC was added and mixed gently to achieve a slurry composition with 30% solids by weight. The mixing continued until homogeneity was achieved (usually after approximately 1 hr.). The electrode slurry was casted onto the current collector with the use of an adjustable micrometer film applicator (AP-99500806) from Paul N. Gardner Company Inc. The electrodes after casting was air dried before annealed in the oven at 130 ºC.

3.2.2 FABRICATION OF MCDI STACK

An MCDI stack with total and effective single electrode area of 20 cm x 9 cm was fabricated for this research. The stack was fabricated to accommodate multiple parallel MCDI cells. Ion exchange membranes (CMX and AMX) with thickness of 0.13 mm were obtained from ASTOM-Neosepta and cut into size (20 cm x 9 cm) for this application. The side view picture of the MCDI stack and dimensions are shown in Figure 3.1 (a) and (b). A photo of the components making up a single MCDI cell is shown in Figure 3.1 (c) with a U.S. quarter dollar for scale. The stack was sealed with Neoprene Rubber (TK19653265T, thickness of 0.74 mm) around the perimeter of the electrodes stack. The stack had a linear flow path with water flowing by the electrodes through a 0.23 mm thick mesh spacer.

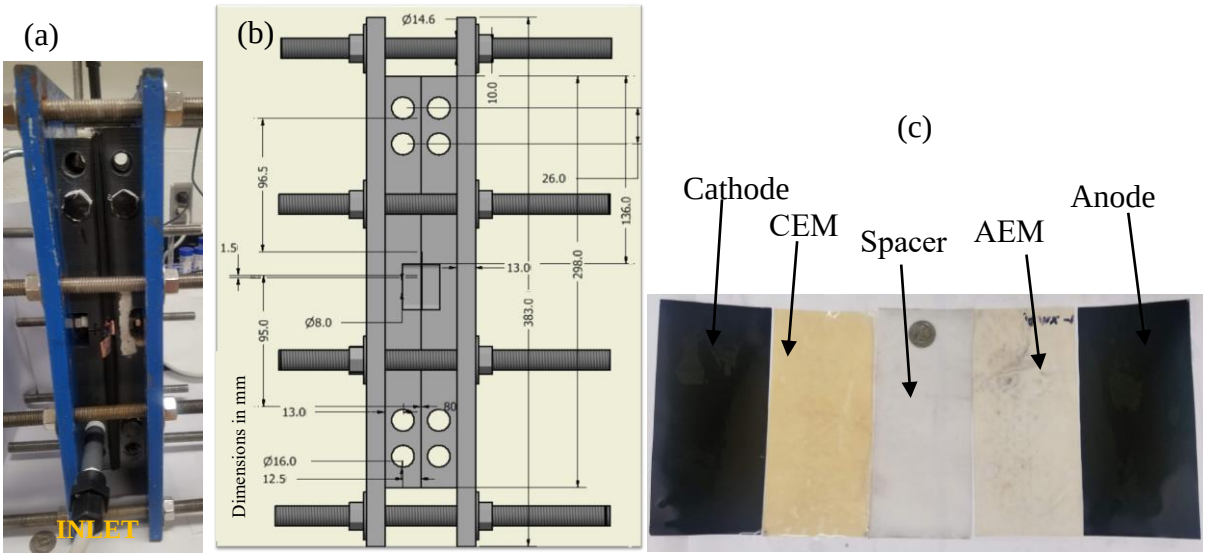

Figure 3.1: (a) Side view of MCDI stack; (b) cross section and dimensions; (c) single cell set up (cathode, cation exchange membrane (CEM), flow spacer, anion exchange membrane (AEM), and anode)

3.2.3 EXPERIMENTAL DESIGN

The experimental MCDI setup, including the supervisory control and data acquisition system (SCADA), was explained in Chapter 1. Experiments were performed with NaCl solutions with electrical conductivity of 3 mS/cm and 5 mS/cm (1569 mg/L and 2622 mg/L, respectively). The experiments were performed with detention times of 12 s, 30 s, 60 s, and 120 s for different number of MCDI cells. Constant voltage (1.2 V) operation was used for all experiments in the sorption (charging or product) phase and the desorption (discharge or concentrate) phase was run by short circuiting the MCDI device.

3.2.4 ANALYSIS AND CALCULATIONS FOR DETERMINING SYSTEM PERFORMANCE

The determination of performance parameters of conductivity reduction (salt removal), charge efficiency, hydraulic recovery, and specific energy consumption (SEC) were explained in Chapter 1. The salt adsorption capacity (SAC, meq/g) for the aqueous processed electrodes was calculated by the following equation.

Equation 3.1 $$SAC = \frac{Q \int_0^t (C_f - C_p(t))dt}{M_{electrode}}$$

where Q is the product phase flow rate, C_f is the concentration of the feed solution (meq/L), $C_p(t)$ is the concentration of the product water at any time, t (s), and $M_{electrode}$ is the mass of the anode and cathode (without the mass of the current collector).

3.3 Results and discussions

3.3.1 SCALED-UP ELECTRODES PERFORMANCE

Electrodes were fabricated as explained in §3.2.1 and SEM images of a sample electrode are shown in Figure 3.2**.** The side view image (Figure 3.2 (a)) clearly shows the electrode slurry cast (left) over the graphite current collector material and the difference in material composition. The top view image for the slurry cast shows a highly porous electrode cast and with different grains sizes.

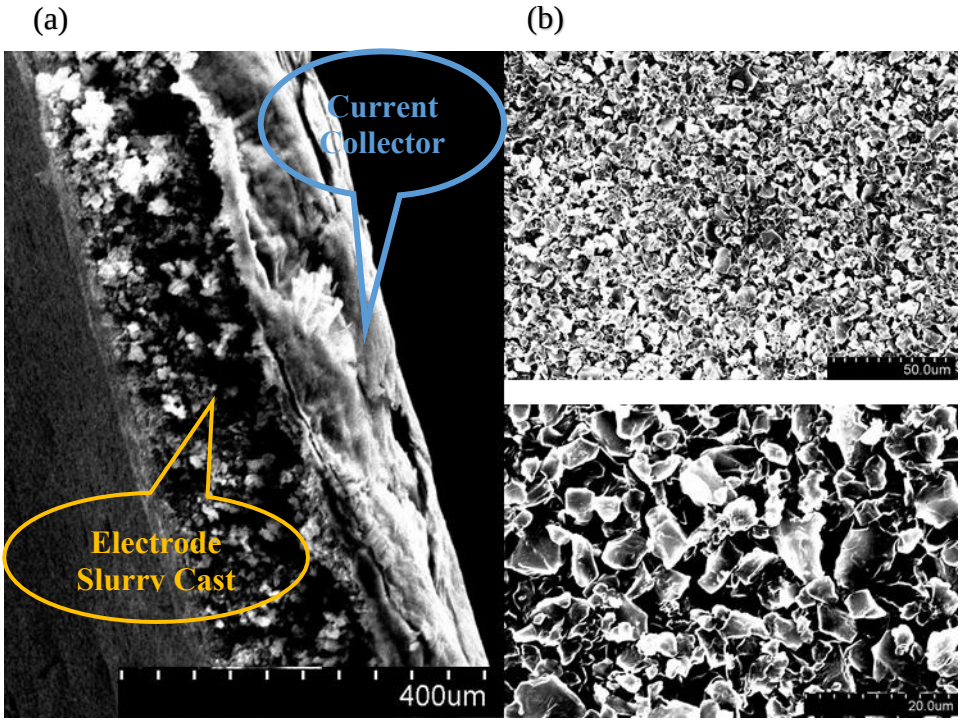

Figure 3.2: (a) SEM side view image of a sample fabricated electrode showing electrode slurry cast over the graphite sheet current collector; (b) top view SEM image at two resolutions

The applicator was set to produce electrode plus current collector thicknesses of 0.35 mm. The electrodes (without the mass of the current collector) weighed an average of 8.3 mg/cm^2. Experiments were performed at constant voltage of 1.2 V with a feed solution of 3 mS/cm or 5 mS/cm sodium chloride with one, four, eight, twelve, and sixteen MCDI cells. Overall, nineteen experiments were performed, and analysis showed an average SAC of 0.413 meq/g with coefficient of variation of 6%. Further details on this analysis is shown in Appendix C.

3.3.2 8-CELL MCDI REACTOR PERFORMANCE

Experiments were performed to show system desalination performance with eight cells (total cell area of 0.128 m^2) and was compared to performance observed for the commercial Voltea VS1 MCDI module (17 cells, total cell area of 0.362 m^2). The maximum conductivity reduction (Maximum Cumulative Removal) achieved in the product phase for the experiments are shown in Figure 3.3 (a). The Voltea MCDI unit (17 cells, 0.362 m^2) was able to achieve a 78% maximum

cumulative removal for the 5 mS/cm solution in comparison to the 60% achieved by the fabricated 8-cell device. The total cumulative conductivity reduction (Total Cumulative Removal) for the 8-cell device for a 3 mS/cm and 5 mS/cm feed, and for a 5 mS/cm feed for the Voltea unit are shown in Figure 3.3 (b). The fabricated MCDI device was able to achieve a highest total cumulative removal of 24% for the full adsorption operation for a 5 mS/cm feed in comparison to the 46% for the Voltea system.

The fabricated 8-cell MCDI device's charge efficiency was observed to depend on operation detention time as discussed in Chapter 1. Independent of a linear or radial flow path and or the ion exchange layer thickness, the charge efficiency for the MCDI devices decreased with increasing detention time as shown in Figure 3.3 (c) and (d). The hydraulic recovery is dependent on the concentrate phase operation mode, and for the experiments shown in Figure 3.4 (a), the 78% hydraulic recovery was achieved by reducing the flow rate in the concentrate phase to one-eighth of the product flow rate. The fabricated MCDI unit was observed to exhibit faster desorption (concentrate phase) kinetics at lower feed salinity (3 mS/cm sodium chloride) and lower detention time operation (Figure 3.4 (a)).

The normalized specific energy consumption (NSEC, kWh/m^3/meq/L removed) was calculated by dividing the SEC by the salt removal measured (meq/L removed). The NSEC observed for all experiments increased with higher detention times but also with the increase in conductivity reduction as shown in Figure 3.4 (d). This research also helped demonstrate that MCDI operation has a greater charge efficiency at lower detention times. As shown in Figure 3.4 (b), a reduction in charge efficiency and increasing the detention time for MCDI operation contributes to higher NSEC. The equivalent SEC values are plotted and shown in Appendix C.

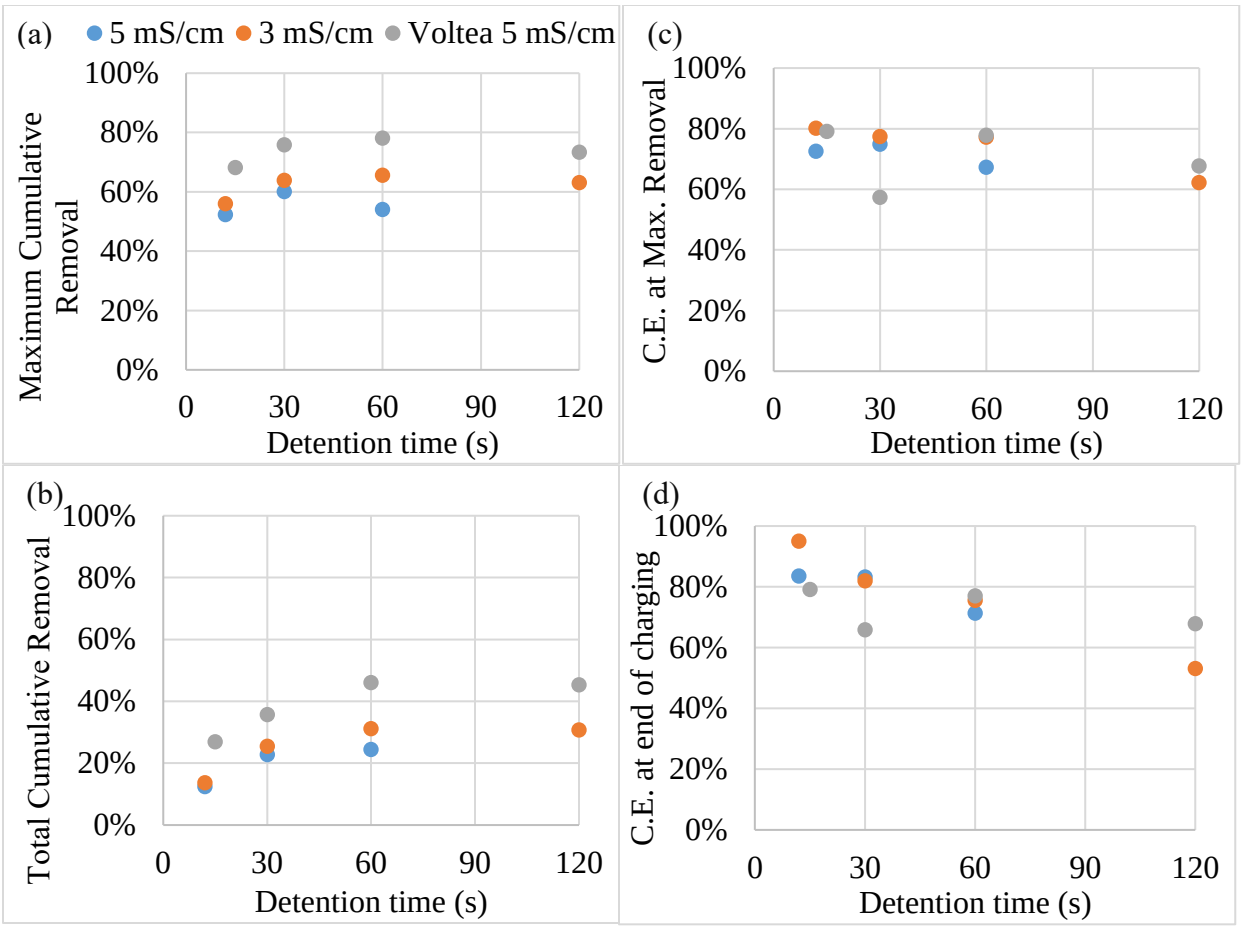

Figure 3.3: Salinity removal at (a) maximum cumulative removal, (b) end of charging (sorption) phase, and Charge Efficiency (C.E.) at (c) the point of maximum removal, and (d) the end of the charging phase. Experiments at 1.2 V constant voltage operation with different sodium chloride feed water conductivity (salinity) and detention times, for an 8-cell laboratory fabricated MCDI device and a Voltea commercial VS1 MCDI unit.

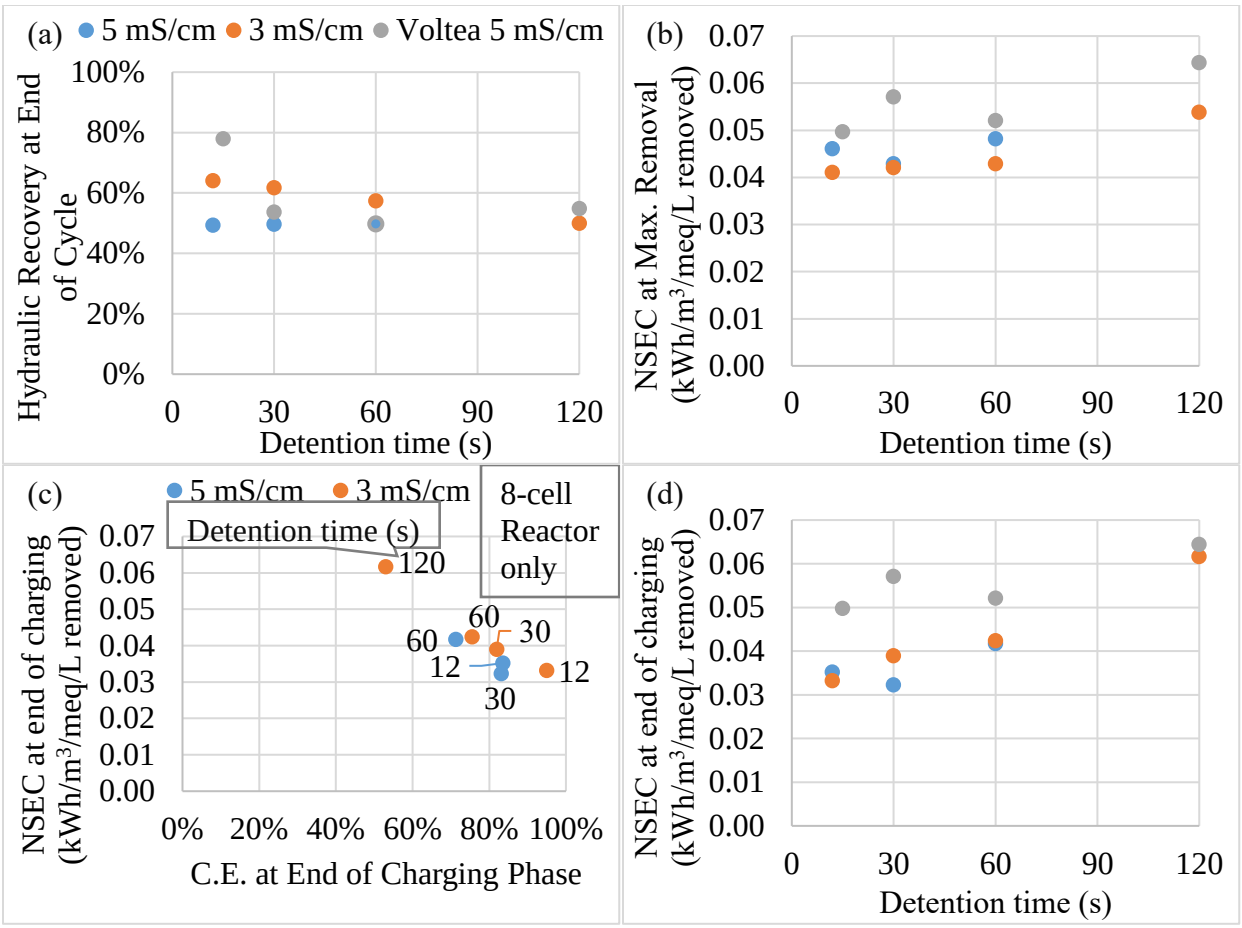

Figure 3.4: (a) Hydraulic recovery at the end of the MCDI cycle, (b) Effect of Charge Efficiency (C.E.) and detention time (data callouts) on the normalized specific energy consumption (NSEC) for an 8-cell MCDI reactor with aqueous processed electrodes, (c) NSEC at the point of maximum cumulative removal and (d) NSEC at the end of charging cycle. Experiments performed at 1.2 V constant voltage operation with different sodium chloride feed water salinities for an 8-cell laboratory fabricated MCDI device and a Voltea commercial VS1 MCDI unit.

3.4 Conclusions

This research successfully showed the fabrication of a bench scale MCDI reactor with capability for multicell operation and up to 16 cells tested. The scale-up of aqueous processed electrodes for MCDI (Jain et al. 2018) was demonstrated at multiple cells with an observed average SAC of 0.413 meq/g (6% coefficient of variation). In comparison to initial small-scale development (SAC of 0.308 meq/g), the aqueous processed electrodes showed good performance.

This research helped to validate the performance of the non-organic solvent based aqueous processed electrodes for MCDI application. This research also helped to reaffirm the effect of the operating detention time condition on the performance of MCDI devices, which has been generally lacking in previous research. as was not previously explained in MCDI research. Overall, the 8-cell MCDI reactor with aqueous processed electrodes was able to achieve a maximum cumulative salinity removal of 60% for a 5 mS/cm (2622 mg/L) sodium chloride solution. This research also demonstrated that the charge efficiency of MCDI operation is greater at lower (<60 s) detention time operations with experiments performed on two different MCDI reactors. The specific energy consumption and the normalized specific energy consumption which significantly affects the operation cost for desalination systems was observed to increase with higher detention times and with the increase in conductivity reduction achieved (salt removal).

GENERAL CONCLUSION

A research evaluation for brackish water desalination by membrane capacitive deionization (MCDI) was performed to show the sensitivity of operating parameters to key desalination performance. Experiments were performed on synthetic and real brackish waters with concentration ranges of 22 meq/L to 98 meq/L (conductivity of 2.5 mS/cm to 10 mS/cm, respectively). Operating voltage application range of 0.4 to 1.2 Volts was used for different MCDI cell configurations. The range of system detention time tested for the MCDI configurations was 6 s to 180 s. The key desalination performance parameters used in this parametric evaluation includes; conductivity reduction (salt removal), charge efficiency, hydraulic recovery, and the specific energy consumption (SEC). Although research has been performed extensively on MCDI there has not been detailed parametric experimental analysis based on the detention time.

The salt removal was observed to increase with the operation detention time and with the voltage application used for the MCDI experiments. Doubling the operating voltage from 0.4 V to 0.8 V at the same detention time for a 5 mS/cm sodium chloride feed solution led to a 10% increase (32% to 42%) in salt removal. The total charging phase salt removal increased from up to 60 s of operating detention time but showed marginal increase with operating detention times greater than 60s. The detention time operation for MCDI was observed to have a negative impact on the system charge efficiency. This is a significant research finding as not previously shown in MCDI research. For the brackish water range tested in this research, a conclusion was drawn on the effect of higher feed water salinity on the charge efficiency. In contrast to earlier discussions in literature, the charge efficiency is negatively impacted by the feed water salinity. Operating at 180 s of detention time, with an applied voltage of 1.2 V, the charge efficiency for feed sodium chloride of 2.5 mS/cm, 5 mS/cm, and 10 mS/cm was 74%, 57% and 50%, respectively.

The hydraulic recovery for MCDI is mainly dependent on the operating conditions used in the concentrate phase. An analysis was done to identify a combination of operation conditions that provides the highest hydraulic recovery for desalination of the KBH feed water. Operating the concentrate phase by a combination of lower flow rate (LF) and a short polarity reversal (PR) period helped achieved hydraulic recovery of 75% for a single pass conductivity reduction of 42%. The charge efficiency resulting from the selected operating conditions had a positive impact on the SEC. The SEC for the highlighted KBH feed water test at 45 s of detention time, 1.2 V applied voltage, 42% conductivity reduction, and 75% of hydraulic recovery was 1.2 kWh/m^3.

The Simplified Randles Circuit (RCR) model with varying resistance due to conductivity changes developed in this research was able to closely predict the performance of MCDI with higher accuracy (*i.e.* lower Root Mean Squared Error) than the Empirical RC circuit or the Empirical RCR circuit models. This research demonstrated charge efficiency predictions based on the RCR model with less than 3% difference between the modeled and predicted charge efficiency. The model was more correlated with lower detention time operations and lower voltage applications.

This research also showed the scale-up of high capacity aqueous processed electrodes for MCDI. In comparison to performance at small scale, the electrodes showed good performance with an average salt adsorption capacity (SAC) of 0.413 meq/g and a 6% coefficient of variation for nineteen experiments reported.

Appendix A

Voltea VS1 MCDI unit residence time distribution and characterization

A residence time distribution (RTD) analysis was performed on the reactor to characterize the reactor using a tanks-in-series (TIS) model and a dispersed-flow-model (DFM). The RTD (or exit age distribution, *E*) describes the probability distribution of the time it takes for a fluid element to exit from the reactor. Step tracer experiments were performed at different flow rates (detention times) and analyzed to produce a cumulative distribution, *F*, curve. Both the TIS and DFM models were developed using nonlinear regression to fit the number of tanks or dispersion number, respectively, and the mean hydraulic detention time ($\bar{t}$). The TIS model was developed based on the following equation of *F* for series of completely mixed reactors:

Equation A.1
$$F(t) = 1 - exp\left(-\frac{Nt}{\bar{t}}\right) - \frac{Nt}{\bar{t}} exp\left(-\frac{Nt}{\bar{t}}\right) - \frac{1}{2!}\left(\frac{Nt}{\bar{t}}\right)^2 exp\left(-\frac{Nt}{\bar{t}}\right) - \cdots - \frac{1}{(N-1)!}\left(\frac{Nt}{\bar{t}}\right)^{N-1} exp\left(-\frac{Nt}{\bar{t}}\right)$$

where *N* is the number of tanks in series, *t* is the time, and $\bar{t}$ is the mean hydraulic detention time of the complete tank (Benjamin and Lawler 2013). DFM model development was performed with the integration of the exit age distribution $E\left(\frac{t}{\bar{t}}\right)$ equation to generate an $F\left(\frac{t}{\bar{t}}\right)$ equation. The $E\left(\frac{t}{\bar{t}}\right)$ equation used is for low dispersion systems and is shown below.

Equation A.2
$$E\left(\frac{t}{\bar{t}}\right) = \frac{1}{\sqrt{4\pi\left(\frac{1}{Pe}\right)}} e^{-Pe\left(1-\left(t/\bar{t}\right)\right)^2/4}$$

where Pe is the Peclet number, $\bar{t}$ represents the calculated mean hydraulic residence time (Benjamin and Lawler 2013). A section of the system that consists only of flow tubing is modeled

as an ideal plug flow reactor (PFR) with a volume of 60.2 mL, and the theoretical detention time (τ) of the reactor is based on the MCDI unit effective volume of 32 mL.

The $F(t)$ responses for the five flow rates (theoretical detention times (τ)) are shown in Figure A.1 (a) and (b) for TIS and DFM, respectively. The higher flow rate operation behaved more like an ideal plug flow reactor than the lower flow rate operations.

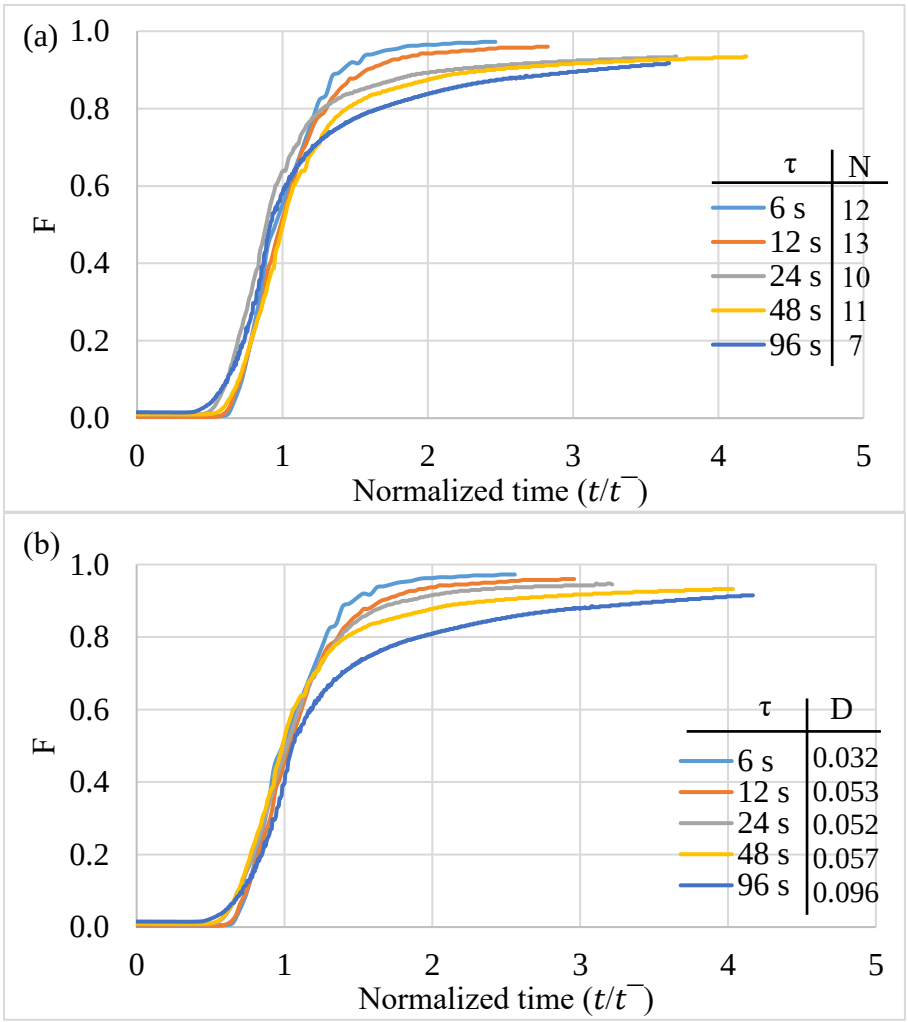

Figure A.1: F curves for five detention times for the Voltea VS1 MCDI unit based on (a) TIS model for $\bar{t}$ and (b) DFM model for $\bar{t}$

Appendix B

The summary of all 17 experiments and Chapter 2 model performance is shown in Table B.1:

Table B.1: RCR varying R1 model results summary for 17 experiments with the Voltea VS1 MCDI module

Experiment	Operation[4] Parameters	A (Ω)	B (cm^{-1})	Capacitance Predicted (Farads)	R_2 (Ω)	Charging Time (min)	Capacitance predicted vs Capacitance measured difference	Charge Efficiency Modeled	Charge Efficiency Prediction Difference	Current Density Prediction RMSE
1	1.2,180,10	0.0001	0.0118	549	1.91	39	-34%	0.49	1%	0.84
2	0.8,180,5	0.0001	0.0053	228	1.59	27	-66%	0.55	0%	0.50
3	1.2,180,5	0.0001	0.0040	180	2.63	41	-78%	0.55	2%	0.78
4	1.2,45,5	0.1089	0.0074	1572	3.17	16	58%	0.63	-3%	0.68
5	1.2,120,5	0.0361	0.0001	186	1.95	35	-79%	0.66	0%	0.86
6	0.5,120,5	0.0001	0.0069	389	1.16	11	-39%	0.65	3%	0.26
7	1.2,30,5	0.0593	0.0066	1551	2.07	13	40%	0.66	2%	0.55
8	0.4,180,5	0.0001	0.0083	433	1.83	16	-29%	0.72	0%	0.19
9	1.2,180,2.5	0.1014	0.0002	55	3.94	77	-93%	0.73	0%	0.44
10	1,12,6	0.0227	0.0038	1097	1.20	6	15%	0.76	-2%	0.28
11	1.2,15,5	0.0119	0.0064	1440	1.44	9	27%	0.76	2%	0.42
12	1.2,60,5	0.0009	0.0187	1454	1.45	21	34%	0.79	0%	1.00
13	1,60,5	0.0000	0.0126	1475	0.73	14	40%	0.84	-2%	1.07
14	1,12,3	0.0550	0.0025	1149	1.30	9	15%	0.83	2%	0.40
15	0.5,60,5	0.0001	0.0080	618	0.93	8	-24%	0.85	1%	0.35
16	1,6,3	0.0749	0.0005	979	1.33	8	-2%	0.88	2%	0.29
17	0.5,12,3	0.0916	0.0005	726	1.53	7	-3%	0.95	1%	0.11

[4] Applied Voltage (V), Detention time (s), Sodium Chloride feed conductivity (mS/cm)

Appendix C

Details on aqueous processed electrodes performance at different number of cells with 3 mS/cm and 5 mS/cm sodium chloride feed solution, and constant voltage of 1.2 V are shown in Figure C.1. For the nineteen experiments shown the average salt adsorption capacity (SAC) was 0.413 meq/g with coefficient of variation of 6%.

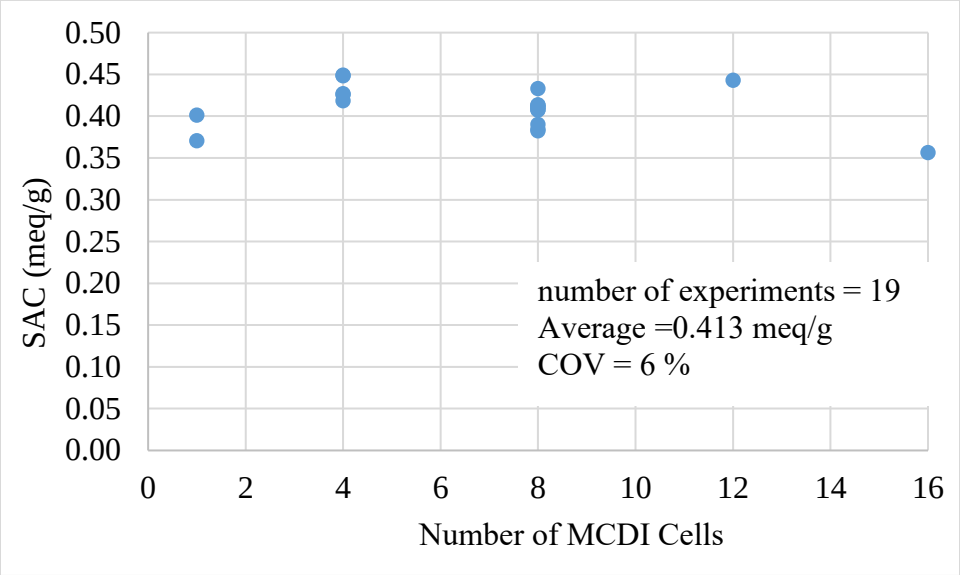

Figure C.1: Average salt adsorption capacity for laboratory fabricated aqueous processed electrodes at 20 cm x 9 cm size.

Figure C.2: Microfilm applicator and freshly casted electrode slurry

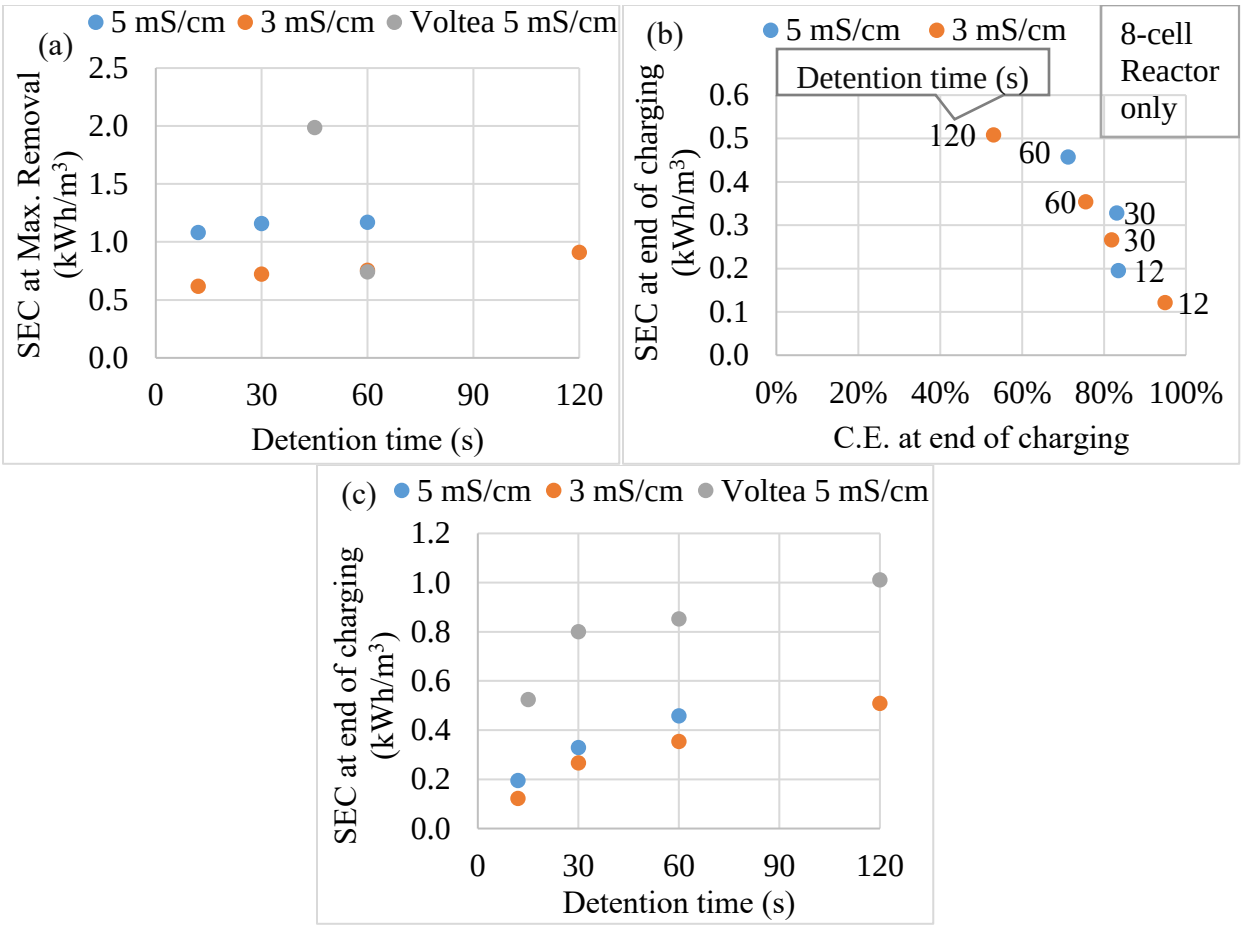

Figure C.3: Specific energy consumption of MCDI experiments performed at 1.2 V for a laboratory fabricated 8-cell MCDI reactor with aqueous processed electrodes and a commercial Voltea VS1 MCDI module with 17 cells; (a) SEC at the point of maximum cumulative removal (b) charge efficiency effect on SEC at the end of charging cycle (c) SEC at the end of charging phase.

References

Anderson, M. A., Cudero, A. L., and Palma, J. (2010). "Capacitive deionization as an electrochemical means of saving energy and delivering clean water. Comparison to present desalination practices: Will it compete?" *Electrochim.Acta,* 55(12), 3845-3856.

Benjamin, M. M., and Lawler, D. F. (2013). *Water quality engineering: Physical/chemical treatment processes.* John Wiley & Sons, .

Bian, Y., Yang, X., Liang, P., Jiang, Y., Zhang, C., and Huang, X. (2015). "Enhanced desalination performance of membrane capacitive deionization cells by packing the flow chamber with granular activated carbon." *Water Res.,* 85 371-376.

Biesheuvel, P., Bazant, M., Cusick, R., Hatton, T., Hatzell, K., Hatzell, M., Liang, P., Lin, S., Porada, S., and Santiago, J. (2017). "Capacitive Deionization--defining a class of desalination technologies." *arXiv Preprint arXiv:1709.05925,* .

Biesheuvel, P., and Van der Wal, A. (2010). "Membrane capacitive deionization." *J.Membr.Sci.,* 346(2), 256-262.

Biesheuvel, P., Zhao, R., Porada, S., and Van der Wal, A. (2011). "Theory of membrane capacitive deionization including the effect of the electrode pore space." *J.Colloid Interface Sci.,* 360(1), 239-248.

Black, J., and Andreas, H. A. (2010). "Prediction of the self-discharge profile of an electrochemical capacitor electrode in the presence of both activation-controlled discharge and charge redistribution." *J.Power Sources,* 195(3), 929-935.

Broséus, R., Cigana, J., Barbeau, B., Daines-Martinez, C., and Suty, H. (2009). "Removal of total dissolved solids, nitrates and ammonium ions from drinking water using charge-barrier capacitive deionisation." *Desalination,* 249(1), 217-223.

Długołęcki, P., and van der Wal, A. (2013). "Energy recovery in membrane capacitive deionization." *Environ.Sci.Technol.,* 47(9), 4904-4910.

Dykstra, J., Zhao, R., Biesheuvel, P., and Van der Wal, A. (2016). "Resistance identification and rational process design in Capacitive Deionization." *Water Res.,* 88 358-370.

Elimelech, M., and Phillip, W. A. (2011). "The future of seawater desalination: energy, technology, and the environment." *Science,* 333(6043), 712-717.

Fritz, P. A., Zisopoulos, F., Verheggen, S., Schroën, K., and Boom, R. (2018). "Exergy analysis of membrane capacitive deionization (MCDI)." *Desalination,* .

Ghaffour, N., Bundschuh, J., Mahmoudi, H., and Goosen, M. F. (2015). "Renewable energy-driven desalination technologies: A comprehensive review on challenges and potential applications of integrated systems." *Desalination,* 356 94-114.

Ghaffour, N., Missimer, T. M., and Amy, G. L. (2013). "Technical review and evaluation of the economics of water desalination: current and future challenges for better water supply sustainability." *Desalination,* 309 197-207.

Greenlee, L. F., Lawler, D. F., Freeman, B. D., Marrot, B., and Moulin, P. (2009). "Reverse osmosis desalination: water sources, technology, and today's challenges." *Water Res.,* 43(9), 2317-2348.

Guyes, E. N., Shocron, A. N., Simanovski, A., Biesheuvel, P., and Suss, M. E. (2017). "A one-dimensional model for water desalination by flow-through electrode capacitive deionization." *Desalination,* 415 8-13.

Han, L., Karthikeyan, K., and Gregory, K. B. (2015). "Energy consumption and recovery in capacitive deionization using nanoporous activated carbon electrodes." *J.Electrochem.Soc.,* 162(12), E282-E288.

He, D., Wong, C. E., Tang, W., Kovalsky, P., and Waite, T. D. (2016). "Faradaic reactions in water desalination by batch-mode capacitive deionization." *Environmental Science & Technology Letters,* 3(5), 222-226.

Hemmatifar, A., Stadermann, M., and Santiago, J. G. (2015). "Two-dimensional porous electrode model for capacitive deionization." *The Journal of Physical Chemistry C,* 119(44), 24681-24694.

Huyskens, C., Helsen, J., and de Haan, A. (2013). "Capacitive deionization for water treatment: Screening of key performance parameters and comparison of performance for different ions." *Desalination,* 328 8-16.

Jain, A., Kim, J., Owoseni, O. M., Weathers, C., Cana, D., Zuo, K., Walker, W. S., Li, Q., and Verduzco, R. (2018). "Aqueous-Processed, High-Capacity Electrodes for Membrane Capacitive Deionization." *Environ.Sci.Technol.,* 52(10), 5859-5867.

Johnson, A., and Newman, J. (1971). "Desalting by means of porous carbon electrodes." *J.Electrochem.Soc.,* 118(3), 510-517.

Kim, J., and Choi, J. (2010). "Fabrication and characterization of a carbon electrode coated with cation-exchange polymer for the membrane capacitive deionization applications." *J.Membr.Sci.,* 355(1-2), 85-90.

Kim, J. S., Jeon, Y. S., and Rhim, J. W. (2016). "Application of poly (vinyl alcohol) and polysulfone based ionic exchange polymers to membrane capacitive deionization for the removal of mono-and divalent salts." *Separation and Purification Technology,* 157 45-52.

Kim, Y., and Choi, J. (2010). "Enhanced desalination efficiency in capacitive deionization with an ion-selective membrane." *Separation and Purification Technology,* 71(1), 70-75.

Lai, J., Karim, Z., Liu, P., and Mathew, A. P. (2018). "Nanocellulose-Based Membranes for Water Purification: Fundamental Concepts and Scale-Up Potential." *Nanocellulose and Sustainability,* CRC Press, 129-146.

Lee, J., Park, K., Eum, H., and Lee, C. (2006). "Desalination of a thermal power plant wastewater by membrane capacitive deionization." *Desalination,* 196(1-3), 125-134.

Lee, J., Bae, W., and Choi, J. (2010). "Electrode reactions and adsorption/desorption performance related to the applied potential in a capacitive deionization process." *Desalination,* 258(1-3), 159-163.

Li, H., and Zou, L. (2011). "Ion-exchange membrane capacitive deionization: a new strategy for brackish water desalination." *Desalination,* 275(1-3), 62-66.

Liu, Y., Pan, L., Xu, X., Lu, T., Sun, Z., and Chua, D. H. (2014). "Enhanced desalination efficiency in modified membrane capacitive deionization by introducing ion-exchange polymers in carbon nanotubes electrodes." *Electrochim.Acta,* 130 619-624.

Mirzadeh, M., Gibou, F., and Squires, T. M. (2014). "Enhanced charging kinetics of porous electrodes: Surface conduction as a short-circuit mechanism." *Phys.Rev.Lett.,* 113(9), 097701.

Mutha, H. K., Cho, H. J., Hashempour, M., Wardle, B. L., Thompson, C. V., and Wang, E. N. (2018). "Salt rejection in flow-between capacitive deionization devices." *Desalination,* 437 154-163.

Omosebi, A., Gao, X., Rentschler, J., Landon, J., and Liu, K. (2015). "Continuous operation of membrane capacitive deionization cells assembled with dissimilar potential of zero charge electrode pairs." *J.Colloid Interface Sci.,* 446 345-351.

Palakkal, V. M., and Arges, C. G. (2017). "Alternative Ion-Exchange Materials for Membrane Capacitive Deionization." *ECS Transactions,* 77(11), 1997-2004.

Porada, S., Borchardt, L., Oschatz, M., Bryjak, M., Atchison, J., Keesman, K., Kaskel, S., Biesheuvel, P., and Presser, V. (2013). "Direct prediction of the desalination performance of porous carbon electrodes for capacitive deionization." *Energy & Environmental Science,* 6(12), 3700-3712.

Porada, S., Zhao, R., Van Der Wal, A., Presser, V., and Biesheuvel, P. (2013). "Review on the science and technology of water desalination by capacitive deionization." *Progress in Materials Science,* 58(8), 1388-1442.

Porada, S., Zhao, R., van der Wal, A., Presser, V., and Biesheuvel, P. M. (2013). "Review on the science and technology of water desalination by capacitive deionization." *Progress in Materials Science,* 58(8), 1388-1442.

Qu, Y., Campbell, P. G., Gu, L., Knipe, J. M., Dzenitis, E., Santiago, J. G., and Stadermann, M. (2016). "Energy consumption analysis of constant voltage and constant current operations in capacitive deionization." *Desalination,* 400 18-24.

Quay, A. N., Tong, T., Hashmi, S. M., Zhou, Y., Zhao, S., and Elimelech, M. (2018). "Combined Organic Fouling and Inorganic Scaling in Reverse Osmosis: Role of Protein–Silica Interactions." *Environ.Sci.Technol.,* 52(16), 9145-9153.

Saleem, M. W., Jande, Y., and Kim, W. (2017). "Performance optimization of integrated electrochemical capacitive deionization and reverse electrodialysis model through a series pass desorption process." *J Electroanal Chem,* 795 41-50.

Saleem, M. W., and Kim, W. (2018). "Parameter-based performance evaluation and optimization of a capacitive deionization desalination process." *Desalination,* 437 133-143.

Subramani, A., and Jacangelo, J. G. (2015). "Emerging desalination technologies for water treatment: a critical review." *Water Res.,* 75 164-187.

Suss, M. E., Baumann, T. F., Bourcier, W. L., Spadaccini, C. M., Rose, K. A., Santiago, J. G., and Stadermann, M. (2012). "Capacitive desalination with flow-through electrodes." *Energy & Environmental Science,* 5(11), 9511-9519.

Suss, M., Porada, S., Sun, X., Biesheuvel, P., Yoon, J., and Presser, V. (2015). "Water desalination via capacitive deionization: what is it and what can we expect from it?" *Energy & Environmental Science,* 8(8), 2296-2319.

Szymczyk, A., Zhu, H., and Balannec, B. (2009). "Pressure-driven ionic transport through nanochannels with inhomogenous charge distributions." *Langmuir,* 26(2), 1214-1220.

Tang, W., He, D., Zhang, C., and Waite, T. D. (2017). "Optimization of sulfate removal from brackish water by membrane capacitive deionization (MCDI)." *Water Res.,* 121 302-310.

Tang, W., Kovalsky, P., Cao, B., and Waite, T. D. (2016). "Investigation of fluoride removal from low-salinity groundwater by single-pass constant-voltage capacitive deionization." *Water Res.,* 99 112-121.

United Nations General Assembly. (2010). "General Assembly Adopts Resolution Recognizing Access to Clean Water, Sanitation as Human Right, by Recorded Vote of 122 in Favour, None against, 41 Abstentions. <http://www.un.org/press/en/2010/ga10967.doc.html> (Jun. 16, 2016)

Wang, M., Xu, X., Li, Y., Lu, T., and Pan, L. (2018). "Enhanced desalination performance of anion-exchange membrane capacitive deionization via effectively utilizing cathode oxidation." *Desalination,* 443 221-227.

Xu, P., Drewes, J. E., Heil, D., and Wang, G. (2008). "Treatment of brackish produced water using carbon aerogel-based capacitive deionization technology." *Water Res.,* 42(10-11), 2605-2617.

Yan, T., Xu, B., Zhang, J., Shi, L., and Zhang, D. (2018). "Ion-selective asymmetric carbon electrodes for enhanced capacitive deionization." *RSC Advances,* 8(5), 2490-2497.

Yang, S., Kim, H., Jeon, S., Choi, J., Yeo, J., Park, H., Jin, J., and Kim, D. K. (2017). "Analysis of the desalting performance of flow-electrode capacitive deionization under short-circuited closed cycle operation." *Desalination,* 424 110-121.

Yao, Q., and Tang, H. L. (2016). "Occurrence of re-adsorption in desorption cycles of capacitive deionization." *Journal of Industrial and Engineering Chemistry,* 34 180-185.

Yu, J., Qin, J., Kekre, K. A., Viswanath, B., Tao, G., and Seah, H. (2014). "Impact of operating conditions on performance of capacitive deionisation for reverse osmosis brine recovery." *Journal of Water Reuse and Desalination,* 4(2), 59-64.

Yu, T., Shiu, H., Lee, M., Chiueh, P., and Hou, C. (2016). "Life cycle assessment of environmental impacts and energy demand for capacitive deionization technology." *Desalination,* 399 53-60.

Zhang, C., He, D., Ma, J., Tang, W., and Waite, T. D. (2018). "Faradaic reactions in capacitive deionization (CDI)-problems and possibilities: A review." *Water Res.,* 128 314-330.

Zhang, J., Hatzell, K. B., and Hatzell, M. C. (2017). "A combined heat-and power-driven membrane capacitive deionization system." *Environmental Science & Technology Letters,* 4(11), 470-474.

Zhang, R., Liu, Y., He, M., Su, Y., Zhao, X., Elimelech, M., and Jiang, Z. (2016). "Antifouling membranes for sustainable water purification: strategies and mechanisms." *Chem.Soc.Rev.,* 45(21), 5888-5924.

Zhao, R., Biesheuvel, P., Miedema, H., Bruning, H., and Van der Wal, A. (2009). "Charge efficiency: a functional tool to probe the double-layer structure inside of porous electrodes and application in the modeling of capacitive deionization." *The Journal of Physical Chemistry Letters,* 1(1), 205-210.

Zuo, K., Kim, J., Jain, A., Wang, T., Verduzco, R., Long, M., and Li, Q. (2018). "Novel Composite Electrodes for Selective Removal of Sulfate by the Capacitive Deionization Process." *Environ.Sci.Technol.,* 52(16), 9486-9494.

Vita

Oluwaseye Michael Owoseni obtained his Bachelor of Engineering degree in Mining Engineering at the Federal University of Technology, Akure, Nigeria in September 2011. He obtained his Master of Science degree in Environmental Engineering in 2016 from UTEP. His academic research works include: a senior capstone project on "Optimization of Drilling and Blasting Operations in Quarries and Mines" and his master's thesis research work on "Analysis of Nitrogen Speciation in Direct Potable Reuse". Seye as fondly called acquired relevant experiences with Archbode Engineering Limited, ENL Consortium Quarry, and the El Paso water utilities during his bachelors and master's degree programs.

His enthusiasm for water treatment and provision of potable water for regions around the globe led him to pursue a PhD degree working on Membrane Capacitive Deionization as part of the NSF Nanotechnology Enabled Water Treatment (NEWT) Engineering Research Center with Rice University, Yale University, and Arizona State University.

Seye plans to work closely with scientists and other engineers in leading processes that efficiently transform nature's raw materials into beneficial products and help to solve industrial and municipal challenges with adequate consideration for the preservation of the environment.

Contact Information: <oaowoseni@gmail.com>